isvr Institute of Sound and Vibration Research

Input Signal Reconstruction for Nonlinear Systems using Iterative Learning Procedures

J.S. Seo and S.J. Elliott

ISVR Technical Memorandum 872

October 2001

University of Southampton

SCIENTIFIC PUBLICATIONS BY THE ISVR

Technical Reports are published to promote timely dissemination of research results by ISVR personnel. This medium permits more detailed presentation than is usually acceptable for scientific journals. Responsibility for both the content and any opinions expressed rests entirely with the author(s).

Technical Memoranda are produced to enable the early or preliminary release of information by ISVR personnel where such release is deemed to the appropriate. Information contained in these memoranda may be incomplete, or form part of a continuing programme; this should be borne in mind when using or quoting from these documents.

Contract Reports are produced to record the results of scientific work carried out for sponsors, under contract. The ISVR treats these reports as confidential to sponsors and does not make them available for general circulation. Individual sponsors may, however, authorize subsequent release of the material.

UNIVERSITY OF SOUTHAMPTON
INSTITUTE OF SOUND AND VIBRATION RESEARCH
SIGNAL PROCESSING & CONTROL GROUP

Input Signal Reconstruction for Nonlinear Systems using Iterative Learning Procedures

by

J.S. Seo and S.J. Elliott

ISVR Technical Memorandum No. 872

October 2001

Acknowledgements

This work is the minor component of grant GR/L62979/01, whose major component was concerned with the adaptive feedforward control of non-stationary systems.

ABSTRACT

This paper demonstrates the reconstruction of input signals from only the measured signal for the simulation and endurance test of automobiles. The aim of this research is concerned with input signal reconstruction using various iterative learning algorithm under the condition of system characteristics. From a linear to nonlinear systems which provides the output signals are estimated in this algorithm which is based on the frequency domain. Our concerns are that the algorithm can assure an acceptable stability and convergence compared to the ordinary iterative learning algorithm.

As a practical application, a ¼ car model with nonlinear damper system is used to verify the restoration of input signal especially with a modified iterative learning algorithm.

CONTENTS

Glossary of Symbols

α	Gain factor
β	Scale parameter for regularisation
δ	Constant (degree of nonlinearity)
ϕ	Phase (degree)
γ_{xy}^2	Coherence function
σ_x^2	Variance of signal x
τ	time sequence
ζ	Damping ratio
c, c_1, c_2	Damping coefficient
$E\{\ \}$	Expectation
E_i	Error at i-th process
f	Frequency
f_s	Sampling frequency
$\hat{G}$	Frequency response function
$h(\tau)$	Impulse response of system
I	Imaginary part
k	Spring constant
M	Magnitude, Mass
n	Number of data points, integer (>0)
N	Total number of data points
$R_y(0)$	Autocorrelation function of observed signal y
R	Real part
S_{xx}	Power spectral density of input signal
S_{xy}	Cross power spectral density

t	Time series (continuous)
t_r	Threshold value
$\mathbf{v}$	Observed (measured) signal vector
$\mathbf{w}$	Noise signal vector
x, x_p	Input signal (time)
X	Input signal (frequency)
y, y_d	Output signal (time)
Y	Output signal (frequency)

1. Introduction

When applying laboratory simulation testing, the test engineer is presented with the problem of reconstructing the service environment in the test laboratory from a set of field measurements (road test data). Since the true configuration of the dynamic behaviour of structure under test (to say 'the system') is not fully identifiable, the reconstruction relies on certain assumptions which must be made about the system. Using a separable set of signals fed to the system, the system is tested to yield an estimate of its linear characteristics, i.e., its frequency response function [1]. This linearly assumed system's frequency response function (hereafter 'estimate of system') is to be used to reconstruct the true excitation in the service environment by comparing the signals measured in the test of laboratory with those from the field measurements [2], [3].

To understand the process of deriving the simulation signals, Figure 1.1 illustrates the overall structure of input estimation from the field measurement.

The major concern in this research is to design the specimen response control system as shown in Figure 1.1. This can be realised by a number of algorithms, which can be classified as using an iterative learning algorithm. This control system then provides an outer control loop among the servo actuator control loop.

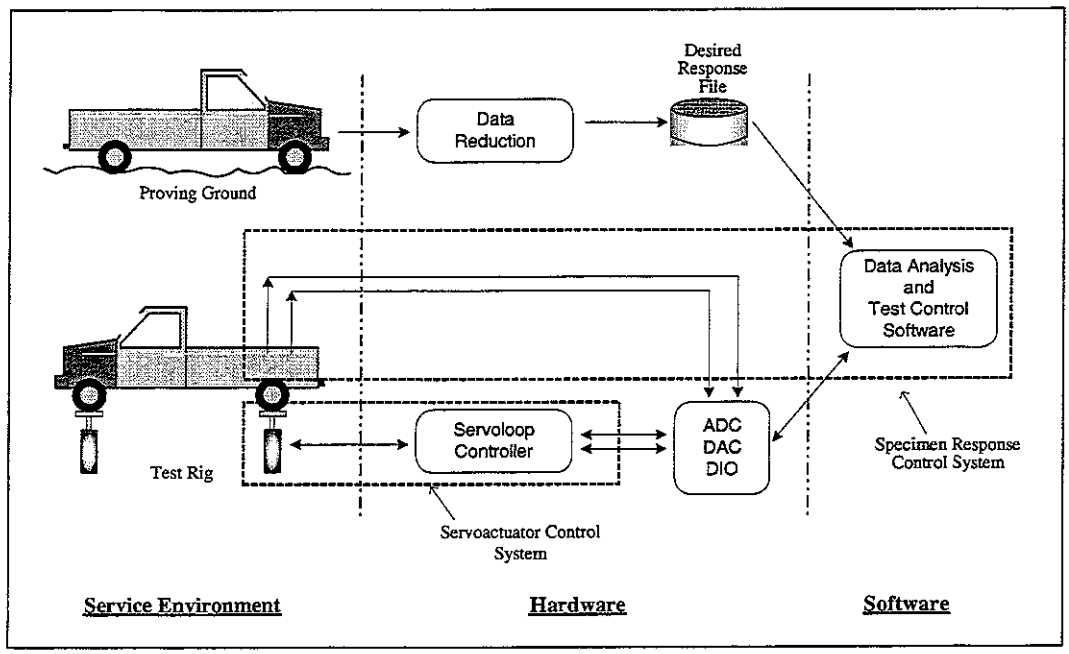

Figure 1.1 Simulation control systems

When the system under consideration is purely linear, the iterative learning procedure is only affected by the accuracy of the estimated frequency response function of the system. However, in practical situations, several types of nonlinearity exist in any mechanical structures, which are usually poorly known. Also these nonlinearities increase with wear and tear, and change from component to component [4], [5], [6], [7].

The aim of this research is concerned with input signal reconstruction using various iterative learning algorithm under the condition of nonlinear system characteristics. Our concerns are that the inverse can exist and stable in applying to the reconstruction.

The underlying theoretical concerns are the adequacy of various models of the nonlinear system, particularly by local linear models, with respect to the convergence of these iterative learning algorithms.

2. Iterative learning algorithm for input estimation

This section mainly focuses on the reconstruction of input signal acting on the linear system. The objective of this section is to provide the general procedure of the iterative learning algorithm including the stability, iteration stop criterion and one sample result of input signal reconstruction based on the frequency domain.

2.1 Input estimation for linear system

In order to understand how the iterative learning algorithm can be applied to simulator control signal generation, a brief review of linear system analysis and its stability condition for the iterative input estimation will help. The information that is needed to construct the true input signal, which is directly related to the control signal, is the relationship between the input and output of a linear system. For a simple example,

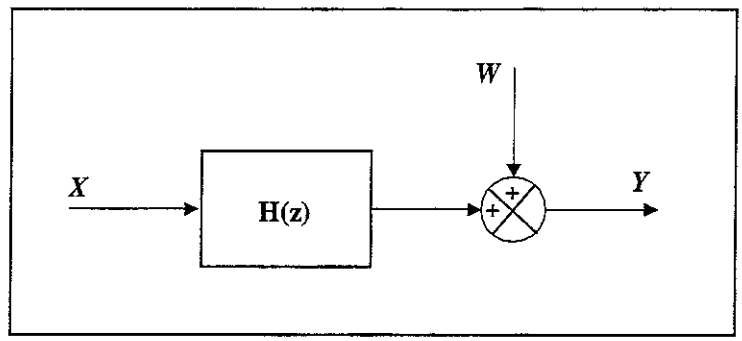

Figure 2.1 Linear system with input-output

Where X is an input, Y is an output, and W is uncorrelated noise.

Based on the least square estimation, the system's frequency response can be estimated as

$$H(f)=\frac{S_{xy}(f)}{S_{xx}(f)} \tag{2.1}$$

where

$$S_{xx}(f)=E\{X(f)^{*}X(f)\}$$
$$S_{xy}(f)=E\{X(f)^{*}Y(f)\}$$

,which is independent of w if it is uncorrelated with x.

Suppose an unknown signal $x_p(t)$ is acting on any linear system $h(\tau)$ producing an output signal $y_d(t)$ (desired output signal) as shown in the following figure;

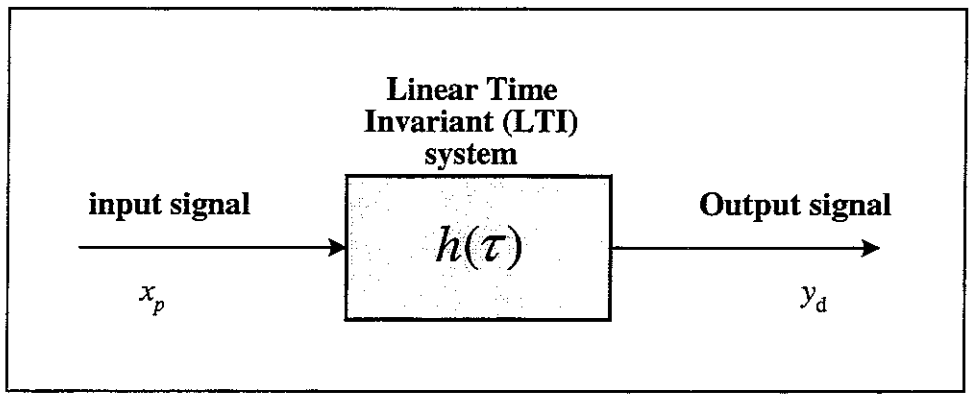

Figure 2.2 Acquisition of desired signal

The problem addressed here is to estimate the unknown input signal from the output and the estimate of the system is linear response. This input reconstruction is achieved in an iterative manner that reducing the error between the desired output and test output obtained from arbitrarily selected input signal excitation.

To be more specific, in the first stage, the system is driven by a test input x_c to give test output y_c, then the system's frequency response is calculated as,

$$\hat{G}(f) = \frac{S_{x_c y_c}(f)}{S_{x_c x_c}(f)} \tag{2.2}$$

Using the frequency response obtained from equation (2.2), the first input x_1, is calculated in the frequency domain as

$$X_1 = \frac{\alpha}{\hat{G}} Y_d \tag{2.3}$$

where Y_d is the desired output signal in frequency domain and α is a gain factor (constant).

Hence, the above relationship may be expressed in general form at the i-th iteration step

$$X_{i+1} = X_i + \frac{\alpha}{\hat{G}} E_i \tag{2.4}$$

and the error in each frequency at every iteration step will be,

$$E_i(f) = Y_d(f) + G(f) \cdot X_i(f) \tag{2.5}$$

where $G(f)$ is the true frequency response of the system.

Figure 2.3 depicts the schematic process of above procedure.

Stage 1 : On site test

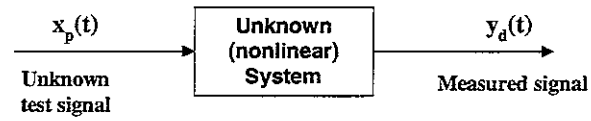

Stage 2 : Lab. simulation

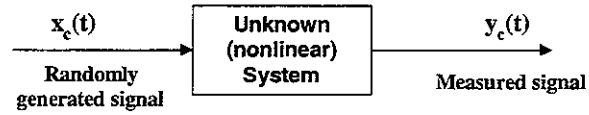

Stage 3 : Estimation of linearly assumed frequency response of system

$$\hat{G}(f) = \frac{S_{X_c Y_c}}{S_{X_c X_c}}$$

Stage 4 : Start adaptation loop

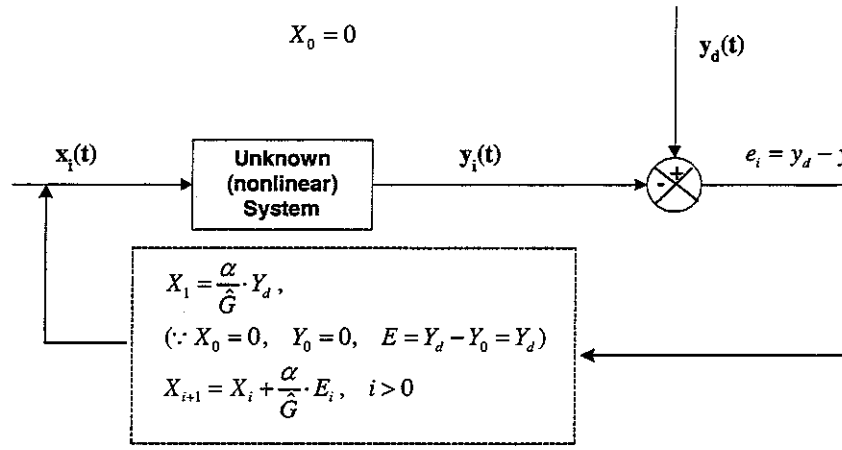

Stage 5 : Unknown test signal (real input) realisation

when $E_i \le t_r$

$$x_{final} \approx x_p$$

Figure 2.3 Iterative learning process for input signal reconstruction

2.2 Stability condition for linear system

In a practical implementation, the transfer function given in (2.2) is not perfect since the system considered here could include some ambiguities due to either the numerical errors in calculating the transfer function or unknown nonlinearities.

The condition for the stability of the iterative learning algorithm described by equation (2.4) can readily be established. Using equation (2.5) for $E_i(f)$ (at the i-th iteration), we can write equation (2.4) as

$$X_{i+1} = X_i + \alpha\left[\frac{Y_d}{\hat{G}} - \frac{G}{\hat{G}}X_i\right] \tag{2.6}$$

where the frequency dependence has been suppressed for brevity, G represents the true frequency response of the system under consideration, $\hat{G}$ is the estimated frequency response and Y_d can be expressed by the relationship between the optimal input estimate and the true transfer function of the system as,

$$Y_d = \hat{G} \cdot X_{opt} \tag{2.7}$$

Substituting (2.7) into (2.6) and subtract a factor X_{opt} from both side of (2.6) yields

$$\left[X_{i+1} - X_{opt}\right] = \left[1 - \alpha\frac{G}{\hat{G}}\right]\left[X_i - X_{opt}\right] \tag{2.8}$$

Thus, for n-th iteration,

$$\left[X_n - X_{opt}\right] = \left[1 - \alpha\frac{G}{\hat{G}}\right]^n\left[-X_{opt}\right] \tag{2.9}$$

From the equation (2.9), the condition for stability is given by,

$$\left|1 - \alpha\frac{G}{\hat{G}}\right| < 1 \tag{2.10}$$

If the real and imaginary part of $\dfrac{G(f)}{\hat{G}(f)}$ are written as $R + jI$, then equation (2.10) can also written as

$$\left|1-\alpha R-j\alpha I\right|^2<1 \tag{2.11}$$

or

$$\left(1-\alpha R\right)^2+\left(\alpha I\right)^2<1 \tag{2.12}$$

so that the condition of α for stability is given by [8]

$$0<\alpha<\frac{2R}{R^2+I^2} \tag{2.13}$$

where

$R=M\cdot\cos\phi$ and

$I=M\cdot\sin\phi$

Assuming the estimation of the system's response can be written as,

$$\hat{G}=M\cdot G\cdot e^{j\phi} \tag{2.14}$$

where M is a positive real number. This implies that the estimated system's transfer function only contains scale and phase ambiguities thus,

$$\frac{G}{\hat{G}}=M\cdot e^{j\phi} \tag{2.15}$$

and so the stability condition given by (2.13) can be written as

$$0<\alpha<\frac{2\cos\phi}{M} \tag{2.16}$$

There are two important points to note about equation (2.16). First, the stability condition can never be fulfilled if $\cos\phi$ is negative, so the algorithm will be unstable unless the phase error in the estimated system's response is less than $\pm 90^\circ$, i.e.

$$\left|\phi\right|<90^\circ, \quad \text{for stability} \tag{2.17}$$

Second, provided the phase condition on $\hat{G}(f)$ is satisfied, any magnitude error can be compensated for by adjusting the magnitude of the convergence coefficient α.

$$\alpha M < 2\cos\phi \tag{2.18}$$

2.3 Examples

Input signal reconstruction for linear system is carried out to introduce the performance of iterative learning algorithm.

Input signal

We selected the input displacement signal as a wideband random signal, generated by passing white *i.i.d* signal (here we selected a Gaussian signal) through an MA filter whose frequency response has pink noise characteristics. The time and frequency shape is given below;

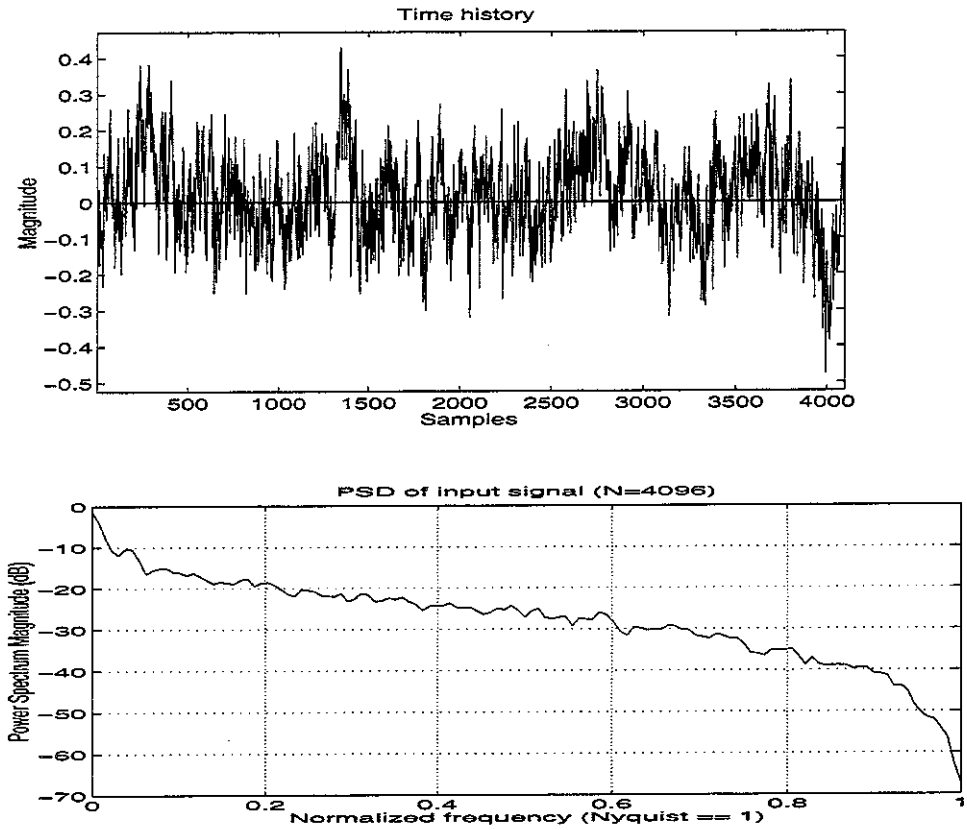

Figure 2.4 Time history and spectral density of input signal

Linear dynamic system

The linear system selected here is assumed to take a second order under damped oscillator whose transfer function is given by

$$H(z)=\frac{1}{\left(z-0.9e^{j\pi/12}\right)\left(z-0.9e^{-j\pi/12}\right)}$$

Pole-zero map of system

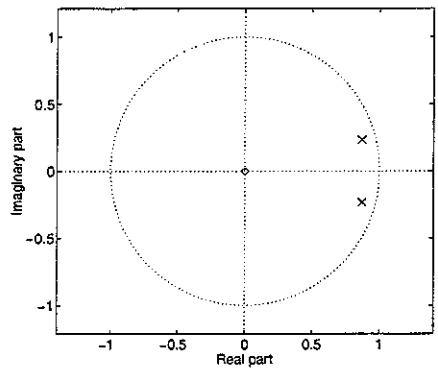

Impulse response of system

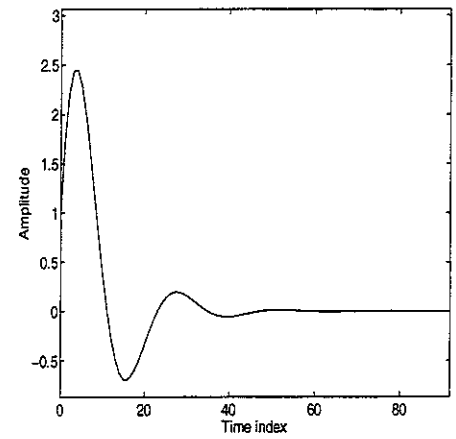

Frequency response of system

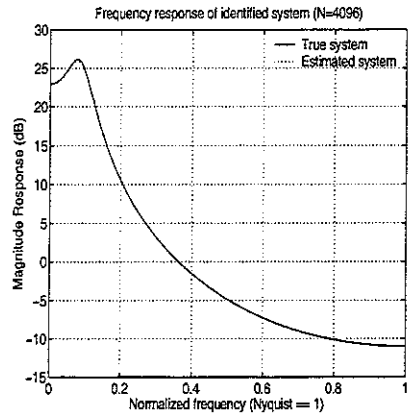

Phase response of system

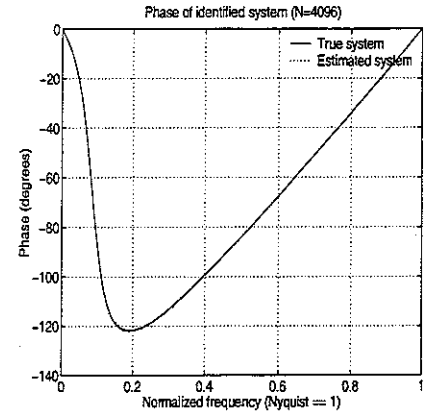

Figure 2.5 Characteristics of selected linear system

Input signal reconstruction (results)

Key parameters;

Sample length (N) : 8192 samples

Sampling frequency (f_s) : 200 Hz

Gain factor (α) : 0.5

Window : Hanning 256 segments

Averaging : 50 % overlapping

Number of iteration : 50

Stability check

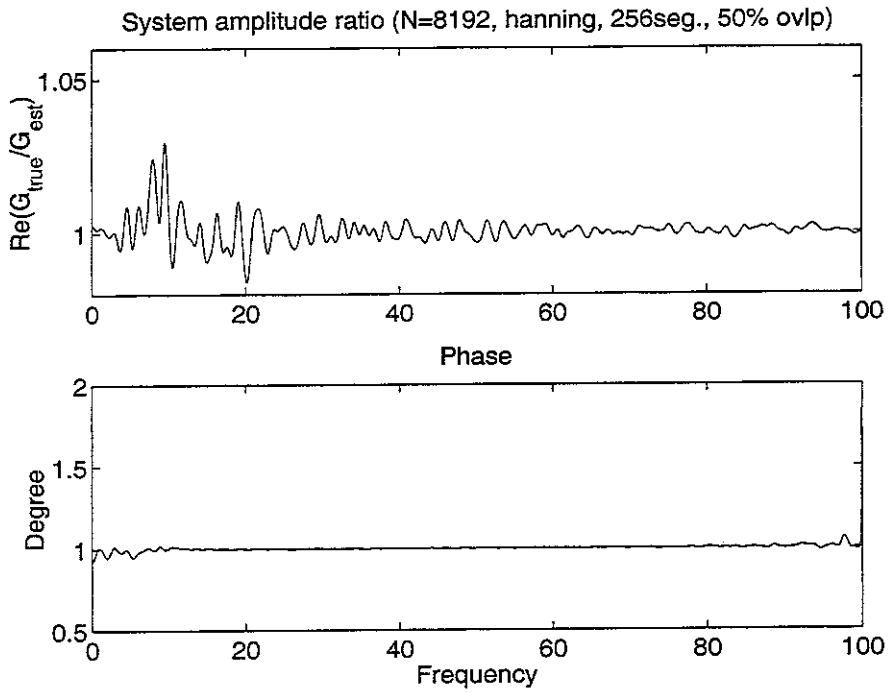

Figure 2.6 Magnitude and phase ratio of the true linear system and estimated linear system

Regarding to the equation (2.17), the phase ratio between the true and estimated frequency response is $|\phi| < 90^\circ$, which assures us the algorithm is always stable.

Iteration stop criterion

The input signal reconstruction does iterate until a certain criterion is met. This criterion (threshold, t_r) is given by a certain number which is compared to the change of magnitude of error (E_i) between two sequent iterations.

$$\left|E_{i-1} - E_i\right| \leq t_r$$

The convergence of error in each iteration is given in Figure 2.7. In this study, the threshold is given by 0.01.

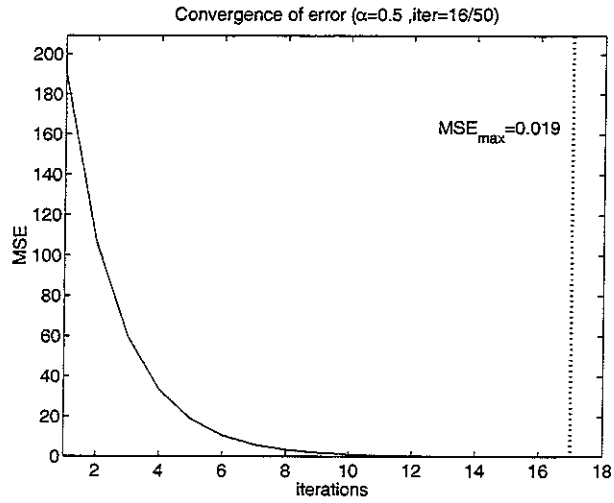

Figure 2.7 Magnitude of error in each iteration

Reconstruction result

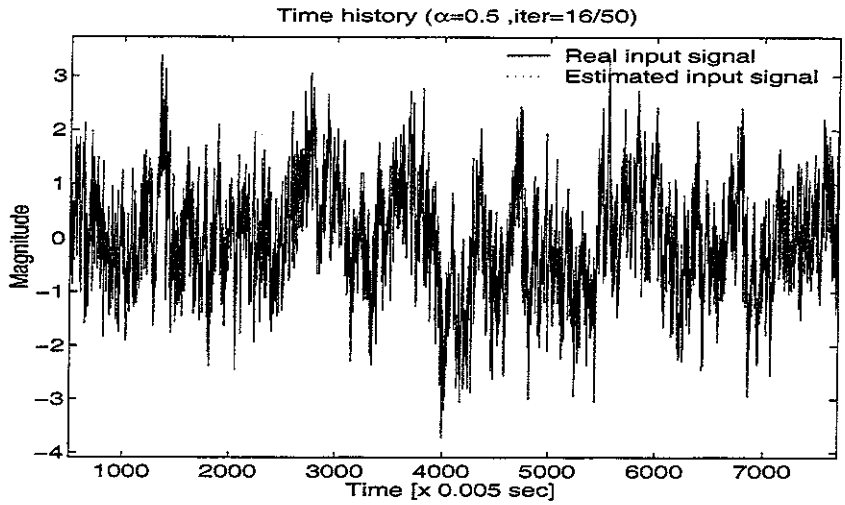

Figure 2.8 Input signal reconstruction

3. Input estimation for nonlinear system

Actuator and sensor nonlinearities are among the key factors limiting the performance of input signal reconstruction. In this section, we applied the iterative learning algorithm to the systems which have nonlinearities in their nature. These system contain not only the static nonlinearities but also dynamic behaviour which can be represented by the 'Hammerstein process' shown as,

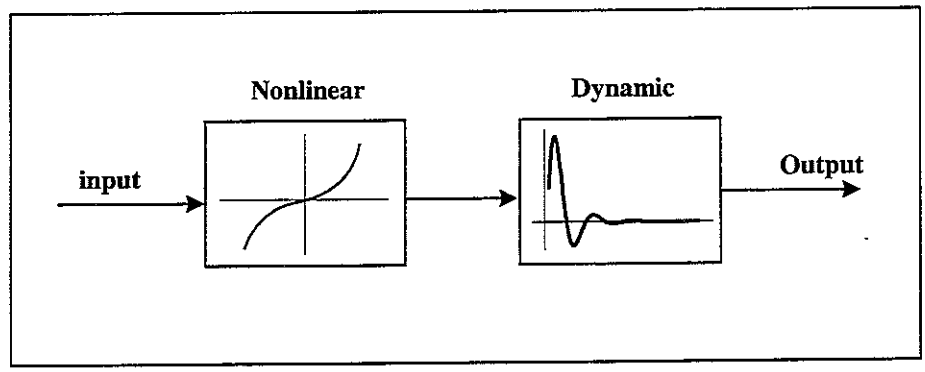

Figure 3.1 Nonlinear dynamic model

Two different nonlinearities are introduced. One of which simply adopt the cubic memoryless nonlinear effect followed by the linear dynamic oscillation used in the previous example. Another is the system with simplest form of hysteresis.

3.1 Stability of the iterative learning algorithm considering the nonlinearity of a system

This section considers the stability of iterative learning algorithm when the system is non-linear. By representing the degree of non-linearity by a single parameter, the region of stability relating the degree of non-linearity and gain factor can be investigated.

The following figure illustrates the relationship between the signals for an iterative learning algorithm in which x denotes the input signal, y is the output of a certain non-linear system, d is the desired signal (field measured output of the non-linear system), and e represents the error signal between the desired and output signals. As a general non-linear expression, we assume the non-linear behaviour of the

unknown system depends on the cubed term of input signal by which the degree of non-linearity can be expressed by a constant multiplier (denoted by δ) of the cubed term.

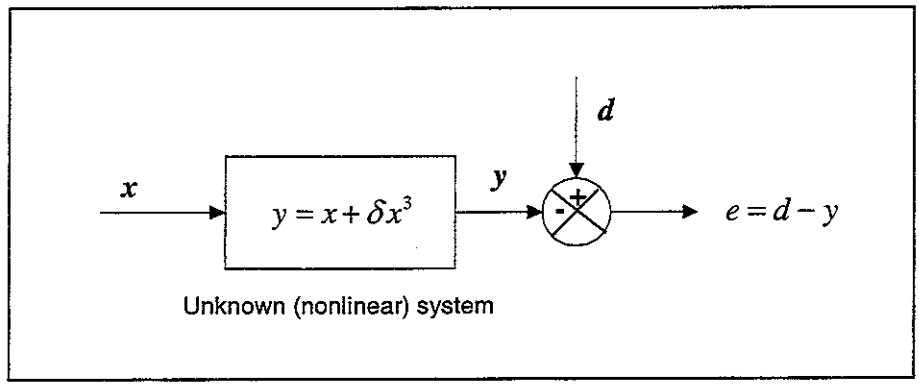

Figure 3.2 Signals and non-linear system used in the iterative learning procedure

Using the relationship of Figure 3.2, the adaptation equation takes the form of

$$x_{i+1}(n) = x_i(n) + \alpha e_i(n), \quad \text{i.e. } \hat{G} = 1 \tag{3.1}$$

in which the error is written as,

$$e_i(n) = d(n) - x_i(n) - \delta x_i^3(n) \tag{3.2}$$

Hence,

$$x_{i+1}(n) = x_i(n) - \alpha\left(x_i(n) + \delta x_i^3(n) - d(n)\right) \tag{3.3}$$

Let $x_{opt} + \delta x_{opt}{}^3 = d$, and substituting x_{opt} from both side of (3.3) becomes

$$\left(x_{i+1}(n) - x_{opt}\right) = \left(x_i(n) - x_{opt}\right) - \alpha\left(x_i(n) + \delta x_i^3(n) - x_{opt} - \delta x_{opt}{}^3\right) \tag{3.4}$$

Normailsing the input signal and convergence gain factor $\tilde{x}_i(n) = x_i(n) - x_{opt}$ and $\tilde{\alpha}_i(n) = \alpha\left[\dfrac{x_i(n) + \delta x_i^3(n) - x_{opt} - \delta x_{opt}{}^3}{x_i(n) - x_{opt}}\right]$ to make equation (3.4) as

$$\tilde{x}_{i+1}(n) = \left(1 - \tilde{\alpha}_i(n)\right)\tilde{x}_i(n) \tag{3.5}$$

Note that the normalised adaptation can be written as $\tilde{\alpha}_i(n) = \alpha\left[1+\delta\left(\frac{x_i^3(n)-x_{opt}{}^3}{x_i(n)-x_{opt}}\right)\right]$.

From this, if $x_i(n)=0$, then

$$\tilde{\alpha}_i(n) = \alpha\left[1+\delta x_{opt}{}^2\right] \tag{3.6}$$

and if $x_i(n) = x_{opt}+\Delta$, $\Delta \ll x_{opt}$, then $x_i^3(n) = \left(x_{opt}+\Delta\right)^3 = x_{opt}{}^3 + 3\Delta x_{opt}{}^2$, so that the normalised convergence coefficient becomes

$$\tilde{\alpha}_i(n) = \alpha\left[1+3\delta x_{opt}{}^2\right] \tag{3.7}$$

From this, the algorithm becomes unstable when

$$\alpha\left[1+3\delta x_{opt}{}^2\right] > 1 \tag{3.8}$$

This equation is exact if x and d are slow-varying dc levels and is true on average if x and d are randomly varying and the mean square value of x_{opt} is used in equation (3.8). Thus, the upper limit of the gain factor for stable convergence becomes

$$\alpha < \frac{1}{1+3\delta x_{opt}{}^2} \tag{3.9}$$

As an example, if we choose δ to be 1.0 and $x_{opt}{}^2$ is taken to be the variance of the signal and assumed to be unity, then the algorithm retains stable for $\alpha \le 0.25$ but when α is taken as 0.5 and $\delta = 1.0$, then the algorithm is driven into the instable condition. A series of simulations has been performed to support this theory, which are reported in Appendix A.

We also notice from Appendix A that the coherence is degraded for a fixed value of δ ($\delta = 1$), as the variance of the input signal, $\sigma_x{}^2$, increases.

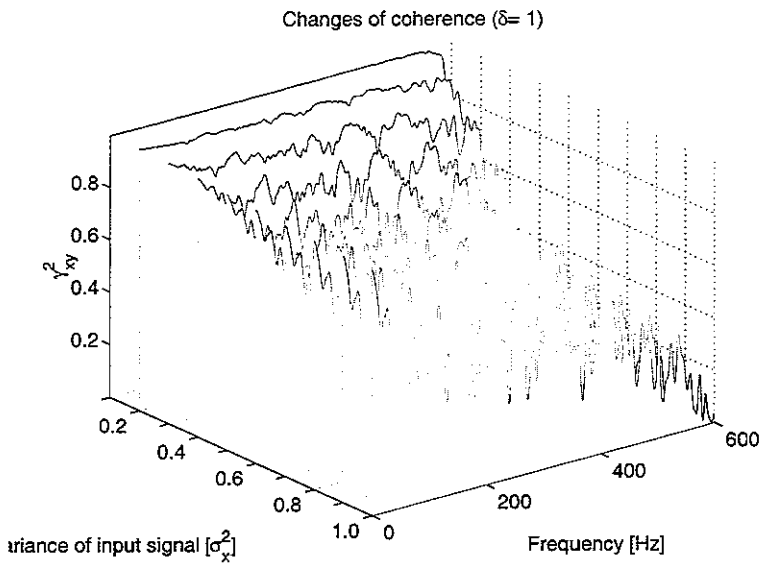

Figure 3.3 Change of coherence varying the variance of input with fixed δ ($\delta = 1$)

It is thus intuitive that by monitoring the coherence function we can monitor the degree of non-linearity in the system experienced by the iterative learning algorithm [2].

In the next Section the form of the coherence function is derived for a general memoryless nonlinearity.

3.2 Analytical form of coherence function

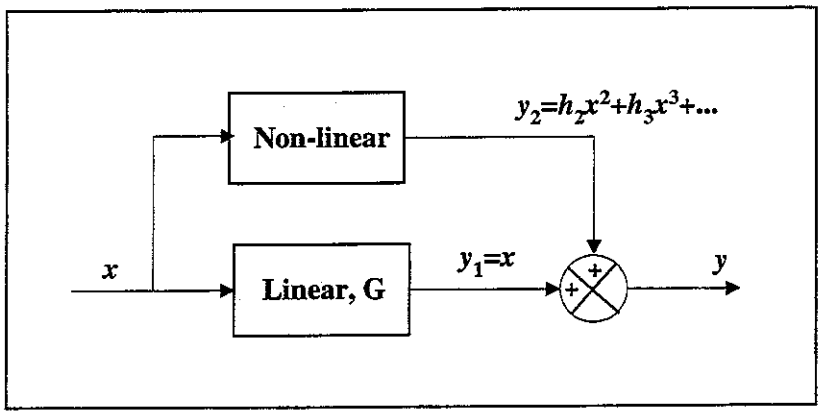

Figure 3.4 A simple parallel non-linear system

The input output relationship can be expressed as

$$y(n) = y_1(n) + y_2(n) \tag{3.10}$$

where $y_1(n) = \sum_{\tau=-\infty}^{\tau=+\infty} h_1(\tau)x(n-\tau)$

and $y_2(n) = \sum_{i=2}^{\infty} \sum_{\tau_1=-\infty}^{\tau_1=+\infty} \sum_{\tau_2=-\infty}^{\tau_2=+\infty} \cdots \sum_{\tau_n=-\infty}^{\tau_n=-\infty} h_i(\tau_1, \tau_2, \ldots, \tau_n)x(n-\tau_1)x(n-\tau_2)\cdots x(n-\tau_n)$.

For simple example, however, we have selected the nonlinear system which is represented as

$$y_2(n) = \delta_1\{x(n)\}^2 + \delta_2\{x(n)\}^3 + \varepsilon\left(x(n)\right)^k, \quad k > 3 \tag{3.11}$$

as such the nonlinear equation given in (3.11) limits the higher order nonlinearity up to 3rd order and the contributions beyond which are considered to be trivial.

The coherence between the input and output is defined to be

$$\gamma_{xy}^{\ 2} = \frac{|S_{xy}|^2}{S_{xx}S_{yy}} \tag{3.12}$$

where

$$\begin{aligned} S_{xy} &= E\{X^*Y\} \\ &= E\{X^*(Y_1 + Y_2)\} \\ &= E\{X^*Y_1\} + E\{X^*Y_2\} \end{aligned} \tag{3.13}$$

and

$$\begin{aligned} S_{yy} &= E\{(Y_1 + Y_2)^*(Y_1 + Y_2)\} \\ &= E\{Y_1^*Y_1\} + E\{Y_2^*Y_1\} + E\{Y_1^*Y_2\} + E\{Y_2^*Y_2\} \end{aligned} \tag{3.14}$$

Since we have assumed that the general non-linear system can be expressed by the relationship given in equation (3.11), the cross spectral density can be expressed using the relationship by the Bussgang process as (for details see Appendix B) [9], [10]

$$S_{xy} = S_{xy_1} + 3\delta_2\sigma_x^2 S_{xx} \tag{3.15}$$

The equation (3.12) becomes

$$\begin{aligned}\gamma_{xy}^{\ 2} &= \frac{|S_{xy}|^2}{S_{xx}S_{yy}} \\ &= \frac{|S_{xy_1} + S_{xy_2}|^2}{S_{xx}(S_{y_1y_1} + S_{y_1y_2} + S_{y_2y_1} + S_{y_2y_2})} \\ &\leq \frac{|S_{xy_1}|^2}{S_{xx}S_{y_1y_1}}\end{aligned} \tag{3.16}$$

in which the equality holds when $\delta_2 = 0$. The inequality relationship given in (3.16) implies that the coherence of the nonlinear system is always less than that of the linear system.

For further detailed non-linear system identification, there can be various ways such as the Higher Order Spectra (e.g. Volterra series expansion) [11], [12], [13] that can deal with the stability of the iterative learning algorithm. In this study, however, the degree of non-linearity is monitored by simple parameter as the cost of iterative learning procedure escalates by implementing further complicated non-linear system identification.

3.3 Further modification of iterative learning process

Apart from the ordinary iterative learning process considered so far, we have introduced a modified iterative learning (IL) process, which takes into account the error signal and system characteristics at each iteration step, to overcome problems encountered in simulating the control of nonlinear systems. This modified IL process has three components.

3.3.1 Estimation using adaptive gain factor application

In the ordinary IL process, the selection of gain factor becomes crucial as the magnitude effects on the stability of the IL process. However, the gain factor is only selected empirically, which may cause unexpected problems in the algorithm if the system is nonlinear as described above. To avoid this, one could let the gain factor change its values in accordance of the coherence function in each frequency. The relationship given equation (3.16) implies that the gain factor can be selected following the change of coherence function in each iteration of the algorithm. To be more specific, we modify the gain factor to tackle the stability of the algorithm in view of the coherence as

$$\alpha_{\text{mod}} = \alpha_0 \cdot \gamma_{xy}^{\,2}, \quad \alpha_0 = 1 \tag{3.17}$$

By considering the status of input and output signal in each iteration (using the coherence function), this equation then suppresses the instability caused by the improperly selected gain factor automatically.

The relationship between the magnitude of gain factor and the stability of the IL process for nonlinear system is tested and summarised in Appendix A.

3.3.2 Instantaneous frequency response function

Instead of using the identified frequency response of system (denoted $\hat{G}$) under test expressed in equation (2.4), the input signal reconstruction is given

$$X_{i+1} = X_i + \frac{\alpha}{\hat{G}_i}(Y_d - Y_i) \tag{3.18}$$

where the estimate of the frequency response function is estimated from the current input and output signals -depending on the status of the phase response of the system in each iteration- using coherence function in each iteration such that

$$\hat{G}_i = \frac{S_{x_i y_i}}{S_{x_i x_i}} \tag{3.19}$$

where $\gamma_{xy}^2 = \frac{\left|S_{x_i y_i}\right|^2}{S_{x_i x_i} \cdot S_{y_i y_i}}$ denotes the coherence function.

For a nonlinear system, the global estimation of frequency response is not always valid as the estimation is based on the linear assumption. Thus, it is recommended to employ the modified frequency response estimation for the input signal reconstruction, which is called 'instantaneous frequency response' estimator.

This frequency response application is used to ensure the rapid convergence of error function and stability in its convergence. Firstly, the merit of this estimation can be said that since the gain factor is varying with the status of the input and output signals in each iteration, γ_{xy}^2 provides an additional gain factor to reduce the error between $(Y_d - Y_i)$. Secondly, the instantaneous linearity can be achieved when we select the local gradient for nonlinear case.

3.3.3 Application of regularisation for inversion of frequency response function

Regularisation is used to ensure numerical stability in the inverse of the frequency response function, i.e.

$$\hat{G} = \frac{S_{xy} + \beta}{S_{xx}} \tag{3.20}$$

in which the small constant β is introduced to ensure the numerical instability of $\hat{G}$ when it is inverted.

Simulations on the inversion of frequency response function on input signal reconstruction have been performed with;

Sample length (N) : 8192 samples with input signal pink noise ($\sigma_x^2 = 1.0$)

Sampling frequency (f_s) : 200 Hz

Window : Hanning 256 segments

Averaging : 50 % overlapping

Number of iterations : 10

System : 8^{th} order Butterworth filter (Cut-off 50 Hz) (memoryless)

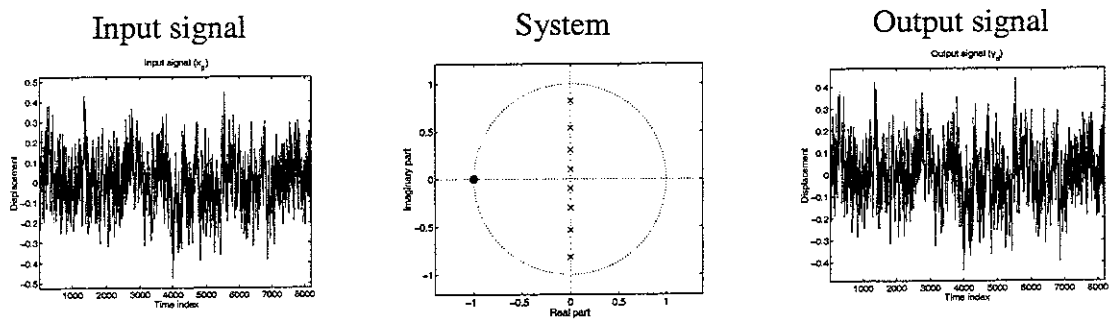

Figure 3.5 Input signal, low pass filter system (memoryless) and output signal

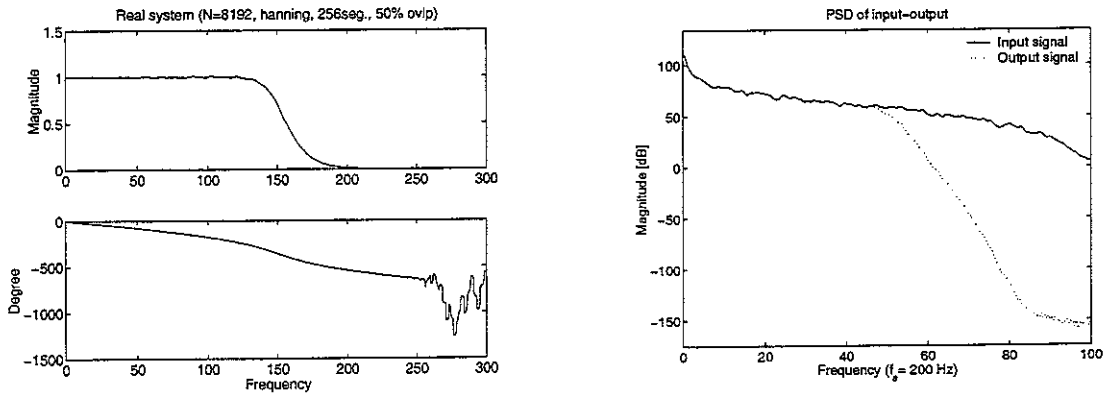

Figure 3.6 Magnitude and phase of the system (left) and spectral density of input and out signal

As shown in Figure 3.6, the system is a kind of low pass filter (left of the figure) which results the output of the system loses its spectral characteristics in high frequency region. In this case, when we invert the frequency response function, the numerical instability occurs.

To compare the performance of the ordinary and modified method in IL process, the term "error" used in this study is represented by MSE, which is defined as

$$\mathrm{MSE} = \sum \left(y_d - y_{a_i} \right)^2 \tag{3.21}$$

where y_d is the measured signal in time domain and y_{a_i} is the i-th output signal respectively.

These are demonstrated in the following figures.

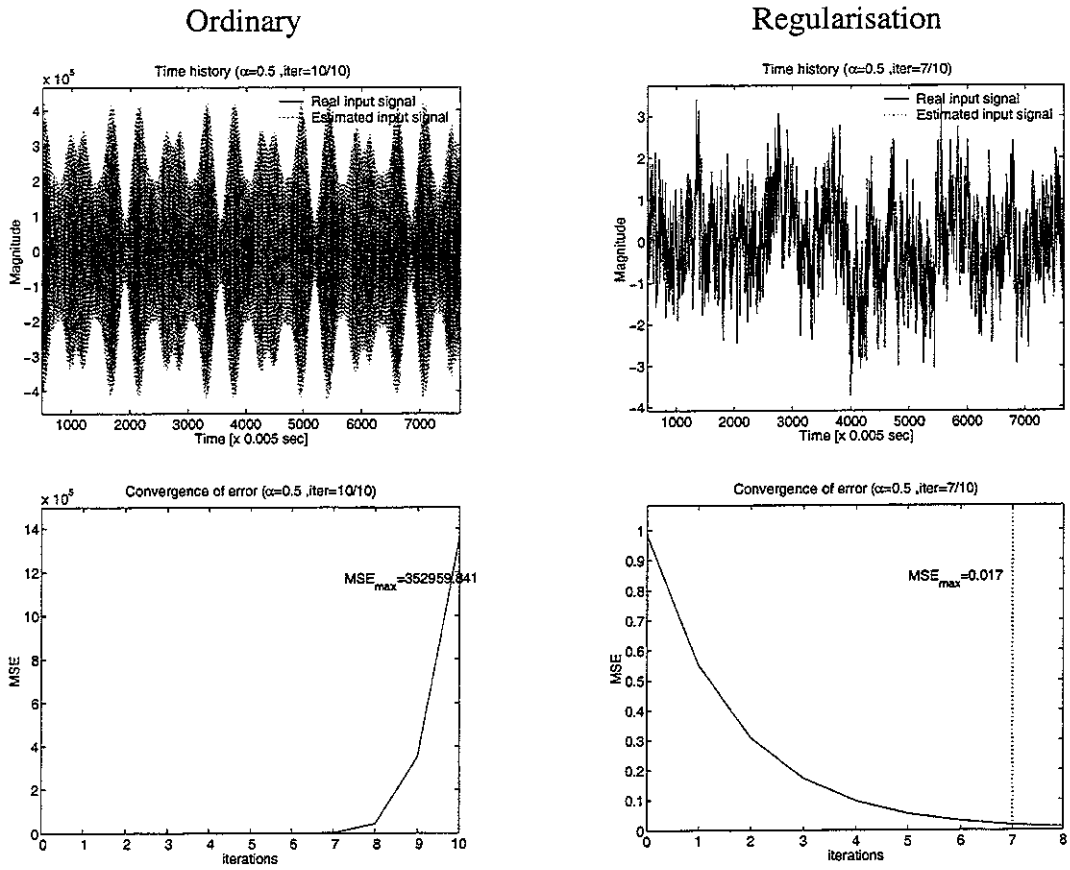

Figure 3.7 Results of input signal reconstruction from three different methods, left : restored signal from ordinary frequency response function inversion, right : from inversion of pre-whitened frequency response function

The left figure of Figure 3.7 clearly demonstrates the numerical instability of the IL process which use only the inversion of the estimated frequency response function as

$$X_{i+1} = X_i + \frac{\alpha}{\hat{G}} \cdot E_i \tag{3.22}$$

whereas the IL process with some constant addition (prewhitening)

$$X_{i+1} = X_i + \frac{\alpha}{\hat{G}(1+\sigma^2 I)} \cdot E_i \tag{3.23}$$

The amount of constant addition is suggested by the Percentage of Pre-Whitening (PPW) and is given ($r_y(0)$ is the auto correlation of the output signal)

$$\text{PPW} = \frac{\sigma^2}{r_y(0)} \times 100 \tag{3.24}$$

and normally, takes $0.5 \sim 5\%$ [14].

The results of input signal reconstruction for ordinary iterative learning algorithm and modified algorithm discussed so far is given in section 3.4.

3.4 Results and comparison

Key parameters;

Sample length (N) : 8192 samples with input signal pink noise ($\sigma_x^2 = 1.0$)

Sampling frequency (f_s) : 200 Hz

Window : Hanning 256 segments

Averaging : 50 % overlapping

Fixed gain factor (α_0) : 0.5

Number of iterations : 10

System : cubic nonlinear (simulation 1) and hyperbolic nonlinear (simulation 2) with dynamics (Hammerstein process)

Simulation 1 : cubic non-linear system

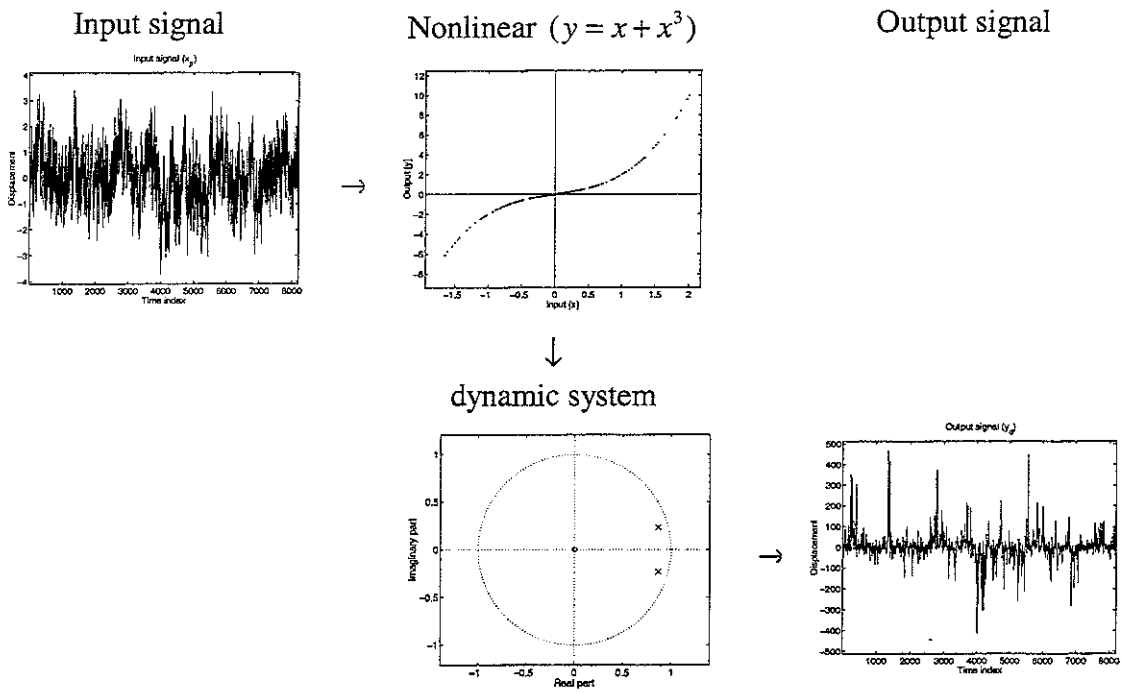

Figure 3.8 Input signal, cubic non-linear system (dynamic) and output signal

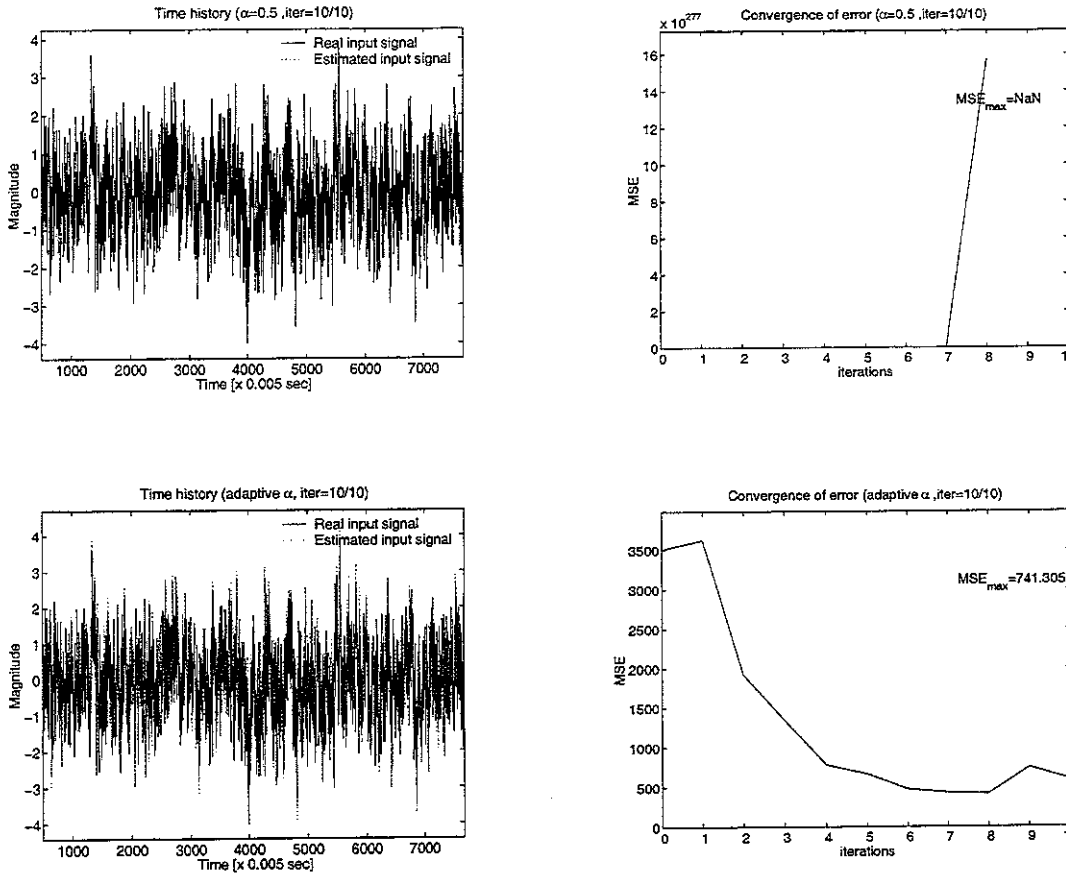

Figure 3.9 Results of input signal reconstruction from two different methods, upper row : restored signal and real input signal (left), errors in each iteration (right) from standard iterative learning algorithm (upper) and from modified gain factor iterative learning algorithm (lower).

Table 3.1 Summary of simulation results

Model	Methods for IL process	Stability	MSE (between input signal and restored signal)	Remarks on the input signal reconstruction
Cubic Nonlinear System	Conventional method	x	-	Unsuccessful
	Modified (new) method	o	0.32	Successful

Simulation 2 : Hyperbolic non-linear system

Input signal Non-linear system Output signal

$$(y = -\tanh(-x \cdot (0.09 - x^2))^2$$

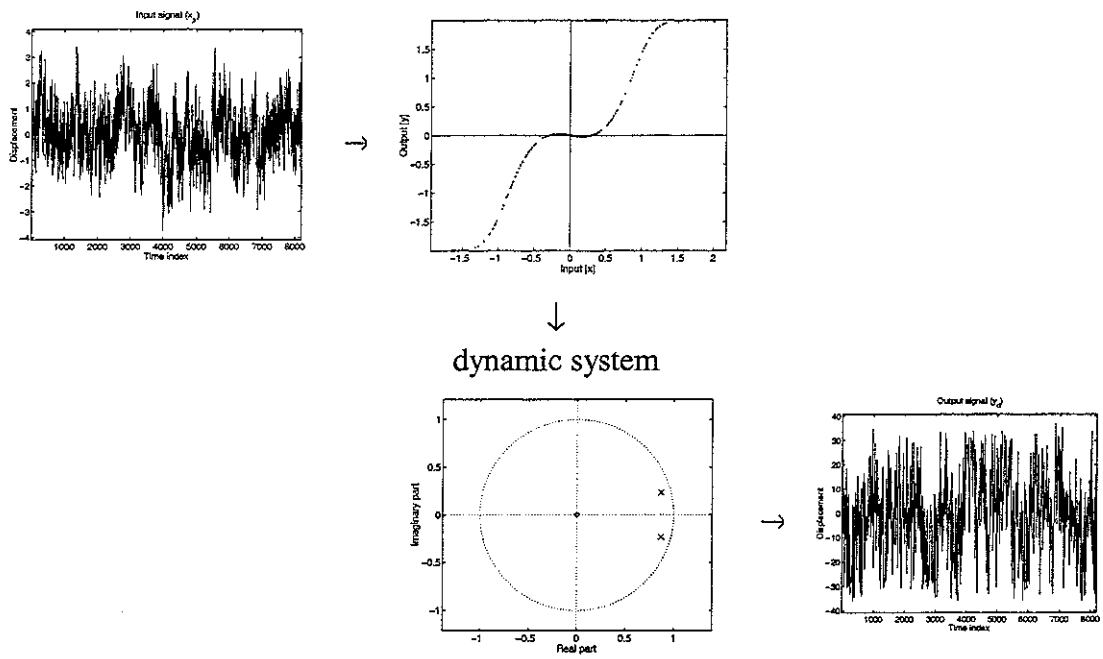

Figure 3.10 Input signal, hyperbolic non-linear system (dynamic) and output signal

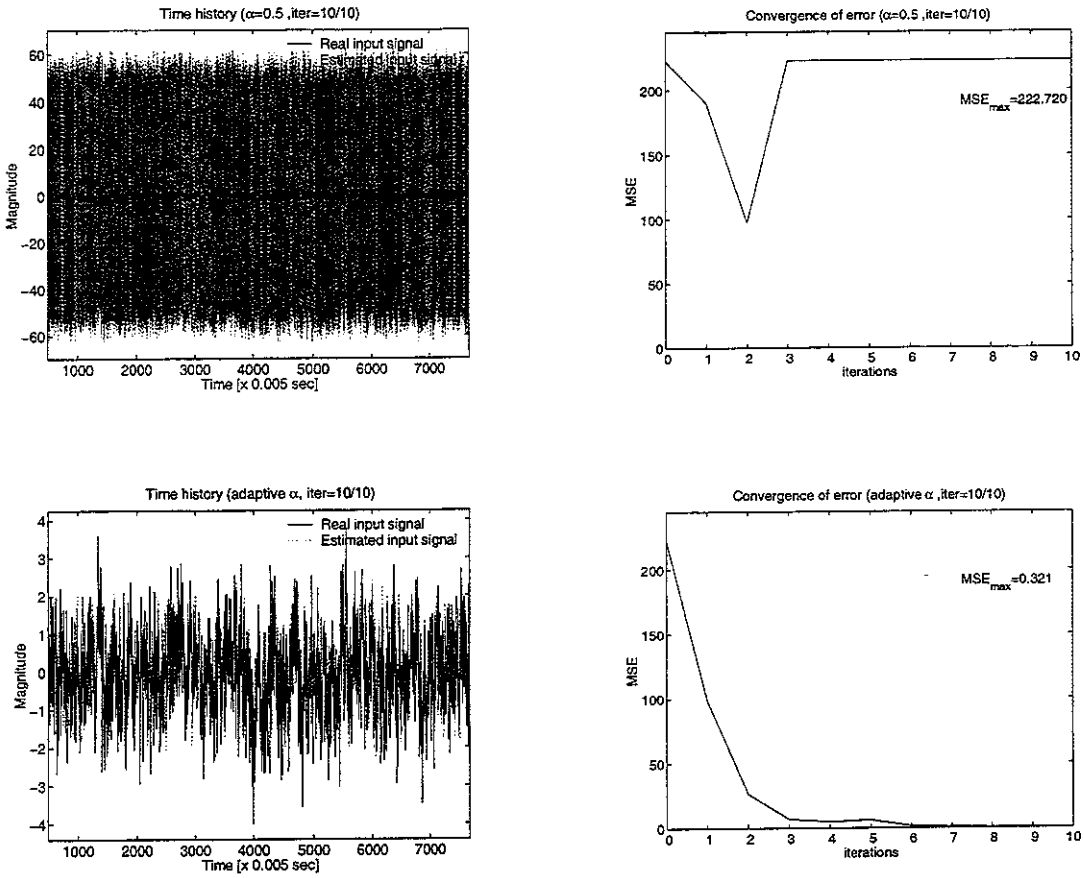

Figure 3.11 Results of input signal reconstruction from two different methods, upper row : restored signal and real input signal (left), errors in each iteration (right) from standard iterative learning algorithm (upper) and from modified gain factor iterative learning algorithm (lower).

Table 3.2 Summary of simulation results

Model	Methods for IL process	Stability	MSE (between input signal and restored signal)	Remarks on the input signal reconstruction
Hyperbolic Nonlinear System	Conventional method	-	2936.39	Unsuccessful
	Modified (new) method	o	0.09	Successful (amplitude of the restored signal is slightly limited)

4. Input estimation for dynamic system with nonlinearity

This section deals with a practical problem of input signal reconstruction by taking a simplified car model with piece-wise nonlinear damper system. The input signal to be restored is the pink noise signal used in previous sections. A brief description of the nonlinear system and the comparison of the input signal construction by the ordinary IL process and modified process are described.

4.1 Input, system, output and analysis of dynamic system

For a practical application of 1/4 car model, nonlinear dynamic system configuration and input estimation processes are given as following;

Key parameters;

M=50kg, c=200N/m/sec, k=1800N/m (f_n=0.955 Hz, ζ=0.333)

Nonlinear damping coefficients : c_1=300, c_2=100 (see right graph of Figure 4.1)

Sample length (N) : 8192, Sampling frequency (f_s) : 200 Hz

Window : Hanning 256 segments, Averaging : 50 % overlapping

Fixed gain factor (α_0) : 0.5

Number of iterations : 10

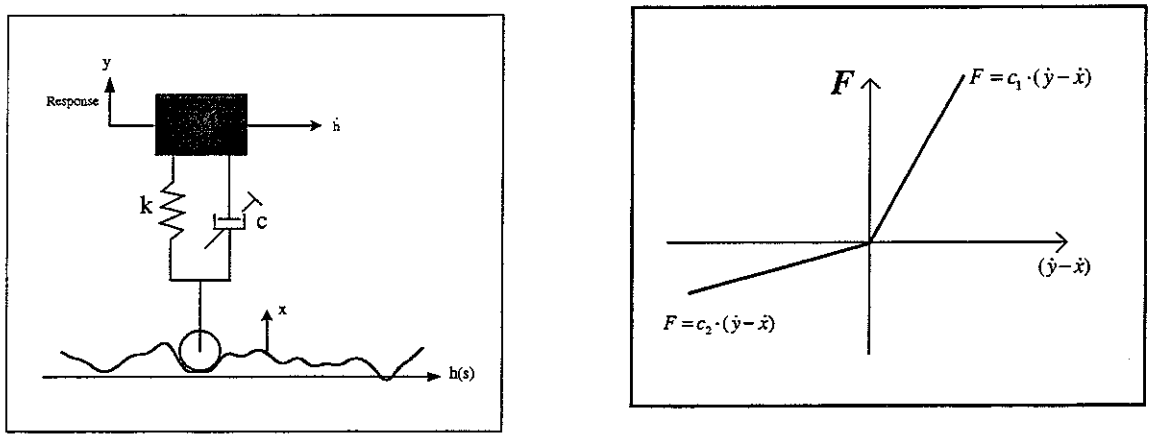

Figure 4.1 Car suspension system (non-linear damper)

The dynamic behaviour of this system becomes

$$
\begin{aligned}
M\ddot{y} &= -k(y-x) - c(\dot{y}-\dot{x}) \\
&\text{when } \dot{y}-\dot{x} \geq 0, \quad c = c_1 \\
&\text{when } \dot{y}-\dot{x} < 0, \quad c = c_2
\end{aligned} \tag{4.1}
$$

In the simulation based on the above equation (4.1), the 4th order Runge-Kutta method has been used to solve the ordinary differential equation. The nonlinear damping coefficient takes either c_1 or c_2 depending on the sign of the relative velocity between the input (road profile) and that of the car body. In this manner, the damping term takes the partial linear behaviour depending on the relative velocity between the input and output.

To solve the ordinary differential equation with random input excitation, an interpolation process has been used to excite the system with correct time sequence.

A sample program counting the partial linear and random excitation is introduced below;

```
function dudt=car_sub_2(t,u)
global dt m c k T N;
load roadinput x
xp=x; x=x(:);
xv=[0; diff(x)];
if t~=0
 dp=N*t/T;
 dl=floor(dp); du=ceil(dp);
 if dl==0
  dl=du;
 end
 Fd=xp(du)+(xp(du)-xp(dl))*(dp-dl);
 Fv=xv(du)+(xv(du)-xv(dl))*(dp-dl);
else
 Fd=xp(1); Fv=xv(1);
end
varc=u(1)-Fv;
if varc>0
 cc=1.5*c;
else
cc=0.5*c;
end
dudt=[-1/m*cc*(varc)+1/m*k*(Fd-u(2)); u(1)];
```

Figure 4.2 depicts signals which represent simple 'vehicle with nonlinear damper system' running over spatially homogeneous rough ground.

Input signal

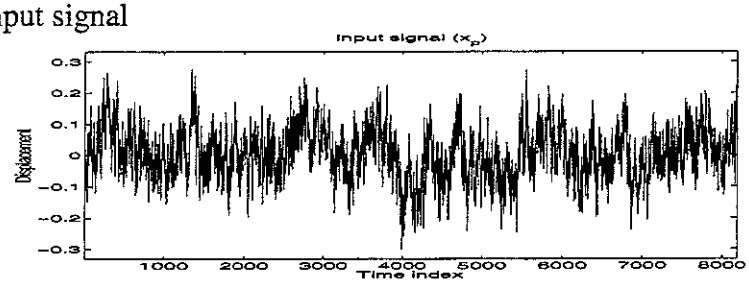

Output from non-linear damper

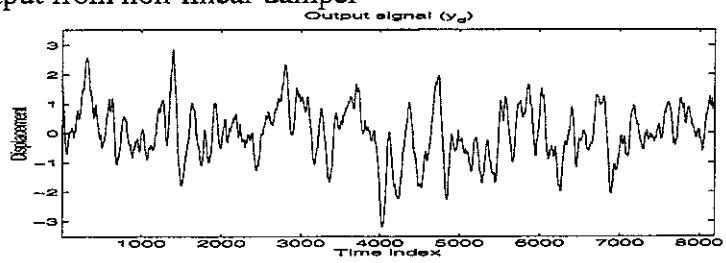

Figure 4.2 Input signal, output signals from non-linear damper car model

Simulation steps;

Step 1 : Any arbitrarily selected random white noise (x_c) is selected to excite the nonlinear car model given in (4.1) to obtain the output of the system (y_c)

Step 2 : The linearly assumed frequency response function of the system ($\hat{G}$) is estimated from the input and output.

Step 3 : The coherence function is estimated to use a modified gain factor for the iteration as such $\alpha_{\text{mod}} = \alpha_0 \cdot \gamma_{xy}^{\ 2}$, $\alpha_0 = 1$.

Step 4 : The spectral differences between the output of the system and the desired output (y_d) as such $E_i = Y_d - Y_a$.

Step 5 : Estimation of frequency response function $\hat{G}$ is done for modified IL process.

Step 6 : A new input signal is then calculated as such $X_{i+1} = X_i + \frac{\alpha}{\hat{G}} E_i$ (where α becomes α_0 or α_{mod} depending on the method selected).

Step 7 : Check the E_i with the threshold value.

Step 8 : If the error E_i is not satisfactory, use the new input to excite the system and repeat from the step 3.

4.2 Results of input signal reconstruction -nonlinear damper car model-

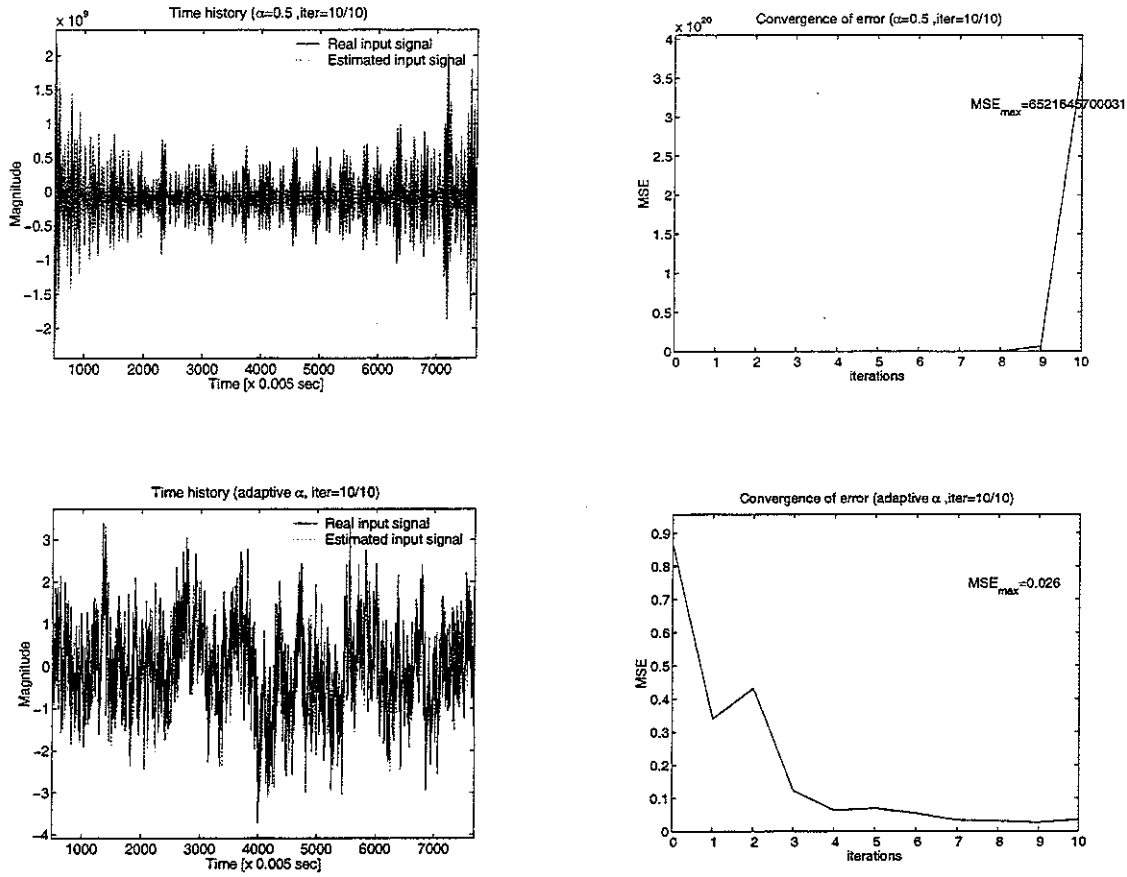

Figure 4.3 Results of input signal reconstruction from two different methods, restored and real input signal (left), errors in each iteration (right) from standard iterative learning algorithm (upper) and from modified gain factor iterative learning algorithm (lower).

As can be seen in Figure 4.3, for the nonlinear case, the input signal reconstruction by two different IL process clearly demonstrate the important role of unknown system's FRF estimation and gain factor selection.

The changes of the system, coherence and error in the inner loop have been plotted in Appendix C.

5. Discussions and future development

The input signal reconstruction using the iterative learning algorithm has been investigated for linear and nonlinear systems. Some of conclusions and further development parts are listed below.

5.1 Discussions

- For linear case, the iterative learning algorithm yields satisfactory and robust results.
- For the simplified car model, using the instantaneous frequency response function, adaptive gain factor and the prewhitening for the inversion stability, the input signal reconstruction has been achieved more effectively, which leaves the following aspects to be further investigated.

5.2 Future development

- A full scale on-site experiment is requires to determine the validity of this process for the real system.
- There is a more general question as to whether an inverse for these nonlinear systems exist and whether it is unique.
- A nonlinear system identification could provide a more accurate input signal reconstruction, which may be achieved using higher order spectra, for example.

6. References

[1] J. F. Fletcher, *Sound and Vibration*, "Global Simulation: New Technique for Multiaxis Test Control", November, 1990.

[2] C. J. Dodds and A. R. Plummer, The Engineering Society For Advancing Mobility Land Sea Air and Space, "Laboratory Road Simulation for Full Vehicle Testing : A Review", SIAT 2001-SAE Conference, 2001-01-0047, Pune, INDIA, 10^{th}-13^{th} January 2001.

[3] S. J. Elliott, *IEEE* Transactions on Signal Processing, "Optimal controllers and adaptive controllers for multichannel feedforward control of stochastic disturbances",
Vol. 48, 1053-1060, 2000.

[4] Gang Tao and Petar V. Kokotovic, *Adaptive Control of Systems woth Actuator and Sensor Nonlinearities*, Wiley Inter-science, 1996.

[5] Darrel Recker and P.V. Kokotovic, *Proceedings of the 32nd IEEE Conference on Decision and Control*, "Indirect adaptive nonlinear control of discrete-time systems containing a dead-zone", pp 2647-2653, 1993.

[6] Darrel Recker, P.V. Kokotovic, D. Rhode and J. Winkleman, *Proceedings of the 30th IEEE Conference on Decision and Control*, "Adaptive nonlinear control of systems containing a dead-zone", pp 2111-2115, 1991.

[7] D. Recker, *Adaptive Control of Systems Containing piecewise Linear Nonlinearities*, Ph.D. Thesis, University of Illinois, Urbana, IL, USA, 1993.

[8] S. J. Elliott, *Signal Processing for Active Control*, Academic Press, 2001.

[9] S. A. Billings and S. Y. Fakhouri, "Identification of nonlinear systems using the Wiener model", *Electronics letters*, 18^{th} August 1977, Vol. 13, No. 17.

[10] J. J. Bussgang, "Correlation Functions of Amplitude-Distorted Gaussian Signals", Tech. Rep. 216, MIT Research Laboratory of Electronics, Cambridge, 1952.

[11] M. Schetzen, *The Volterra and Wiener theories of nonlinear systems*, John Wiley & Sons, 1980.

[12] W. B. Collis, "Higher Order Spectra and their application to Nonlinear mechanical systems", PhD Thesis, ISVR, University of Southampton, UK, 1996.

[13] A. Isidori, *Nonlinear Control Systems, 3rd ed.*, Springer-Verlag, Berlin, 1995.

[14] P. M. Clarkson, *Optimal and Adaptive Signal Processing*, CRC Press Inc., 1993.

Appendix A Effect of the gain factor on input signal reconstruction

Key parameters;

Sample length (N) : 8192 samples with input signal pink noise ($\sigma_x^2 = 1$)

Sampling frequency (f_s) : 200 Hz

Gain factor (α) : 0.05, 0.25, 0.5

Window : Hanning 256 segments

Averaging : 50 % overlapping

Number of iterations : 50

Non-linear system : $y = x + \delta x^3$ with $\delta = 0 \sim 1.0$ (memoryless)

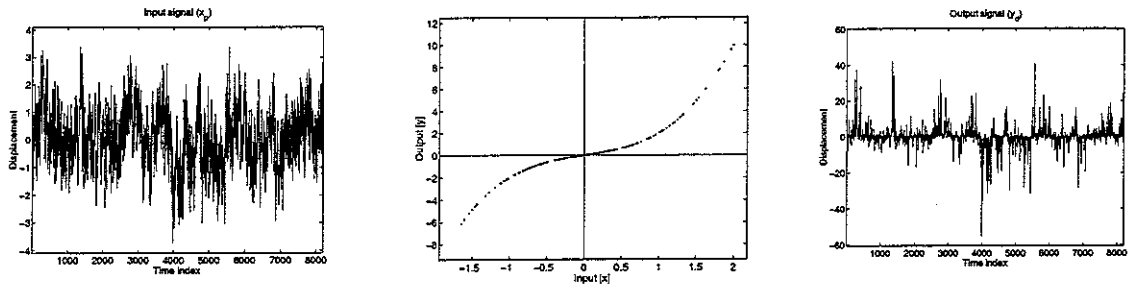

Figure A.1 Input signal, non-linear system and output signal (measured signal)

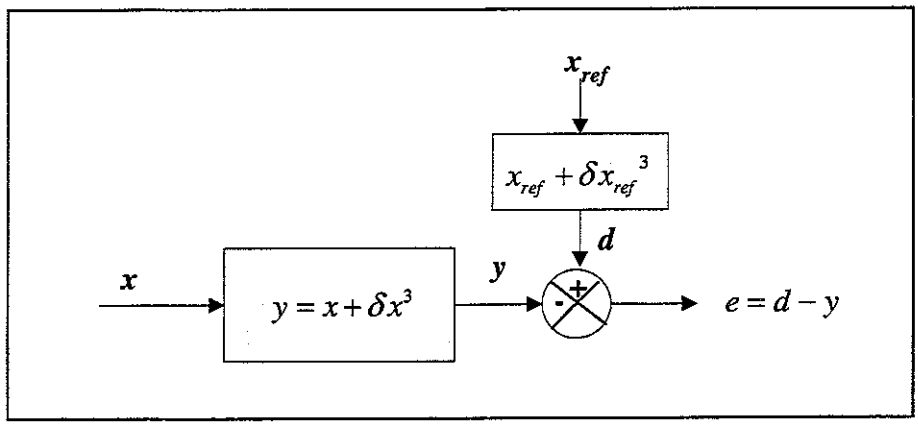

Figure A.2 Input signal reconstruction process for nonlinear system

$$X_{i+1} = X_i + \alpha E_i \tag{A.1}$$

α=0.05 (stable for δ=1)

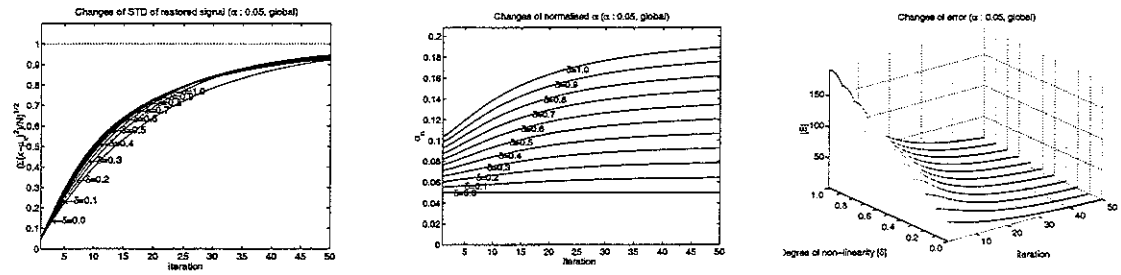

α=0.25 (marginally stable for δ=1)

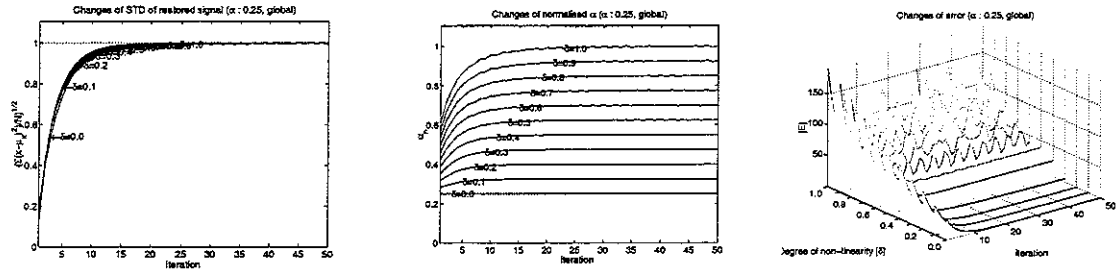

α=0.5 (unstable for δ=1)

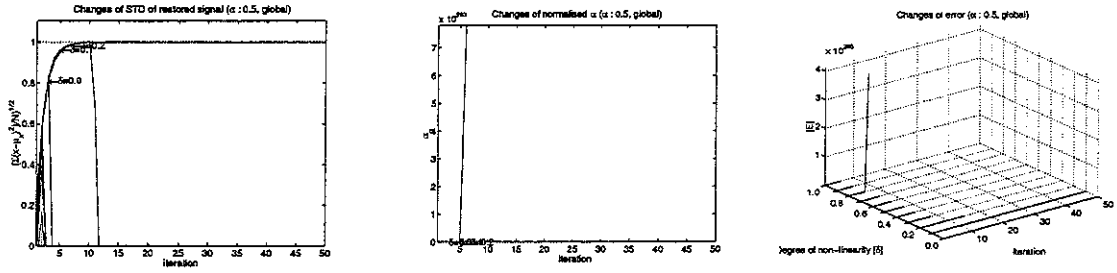

Figure A.3 Change of standard deviation and normalised gain factors with the degree of non-linearity in each iteration for global frequency response estimation

From the results of Figure A.3, we can observe that the stability of the iterative learning algorithm strongly depends on the selection of the gain factor α. This means the gain factor should be appropriately selected to ensure the stability especially for non-linear system.

From numerous simulations, we observed that the stability of this algorithm depends on the magnitude of the input signal (e.g. as the amplitude of input signal becomes bigger than unity, the non-linearity effect increases) as well as the constant multiplier (δ) term of the non-linear part for a fixed gain factor α.

The theoretical gain factor given in equation (3.17) which reflects the variation of the coherence function with the degree of nonlinearity and the simulational gain factor selected from equation (3.18) are compared in the following figure.

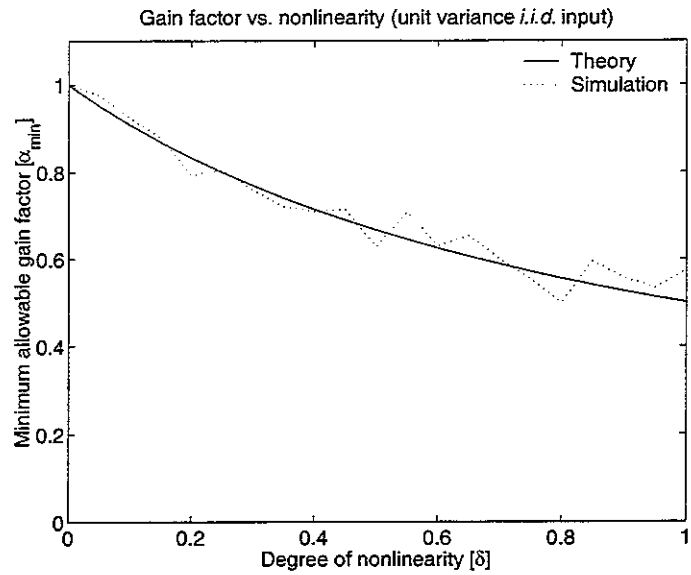

Figure A.4 Change of the minimum allowable gain factor (α) with the degree of non-linearity (δ)

Appendix B Bussgang process and coherence for nonlinear system

For zero-mean *i.i.d.* Gaussian process, the cross-correlation between the input to a memoryless non-linear system and its output have the same shape as the autocorrelation of the inputs.

$$E\{x(n)y(n+\tau)\} = c \cdot E\{x(n)x(n+\tau)\}$$
$$c = \frac{E\{x(n)y(n)\}}{E\{x(n)x(n)\}} \tag{B.1}$$

where $y(n)$ is the output of an arbitrary momeryless non-linear system and we express this in general form

$$y(n) = \delta_1\{x(n)\}^2 + \delta_2\{x(n)\}^3 + \varepsilon\left(x(n)\right)^k, \quad k > 3 \tag{B.2}$$

The cross spectral density is expressed as

$$S_{xy}(f) = \int_{-\infty}^{\infty} E\{x(n)y(n+\tau)\}e^{-j2\pi f\tau}d\tau \tag{B.3}$$

Using (B.1),

$$\begin{aligned} S_{xy}(f) &= \int_{-\infty}^{\infty} E\{x(n)x(n+\tau)\}e^{-j2\pi f\tau}d\tau \cdot \frac{E\{x(n)y(n)\}}{E\{x(n)x(n)\}} \\ &= S_{xx}(f) \cdot \frac{E\{x(n)y(n)\}}{E\{x(n)x(n)\}} \end{aligned} \tag{B.4}$$

The cross correlation term in (B.4) can be rewritten using (B.2),

$$E\{x(n)y(n)\} = \delta_1 E\{x(n)x(n)x(n)\} + \delta_2 E\{x(n)x(n)x(n)x(n)\} \tag{B.5}$$

For zero-mean, *i.i.d.* Gaussian signal $x(n)$,

$$E\{x(n)y(n)\} = 3\delta_2\left(\sigma_x^2\right)^2 \tag{B.6}$$

Thus, (B.4) becomes

$$S_{xy}(f) = 3\delta_2\sigma_x^2 \cdot S_{xx}(f) \tag{B.7}$$

Simulation of the relationship in (B.7) with two different nonlinear systems

Key parameters;

Sample length (N) : 8192 samples with input signal pink and white noise ($\sigma_x^2 = 2$)

Sampling frequency (f_s) : 600 Hz

Window : Hanning 256 segments

Averaging : 75 % overlapping

Non-linear system : $y = \delta_2 x^3$ and $y = \delta_1 x^2 + \delta_2 x^3$ with $\delta_1 = \delta_2 = 1.0$ (memoryless)

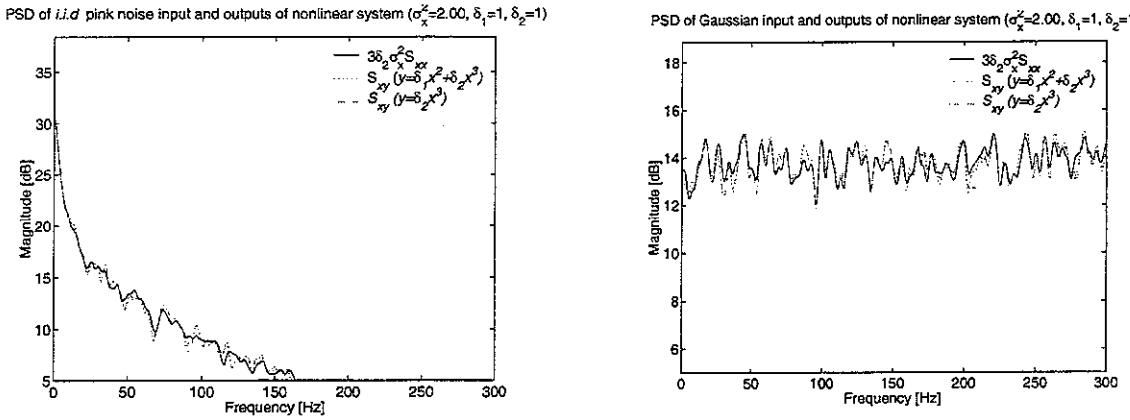

Figure B.1 PSD of Input signal, non-linear system and output signal

Appendix C IL process for non-linear model

C.1 Simulation for nonlinear model

Key parameters;

Sample length (N) : 8192 samples with input signal pink noise ($\sigma_x^2 = 1$)

Sampling frequency (f_s) : 200 Hz

Fixed gain factor (α) : 0.5

Window : Hanning 256 segments

Averaging : 50 % overlapping

Number of iterations : 10

Simulation 1: Changes of frequency response and coherence function for cubic non-linear system ($y = x + \delta x^3$ with $\delta = 1.0$) with dynamics (conventional method)

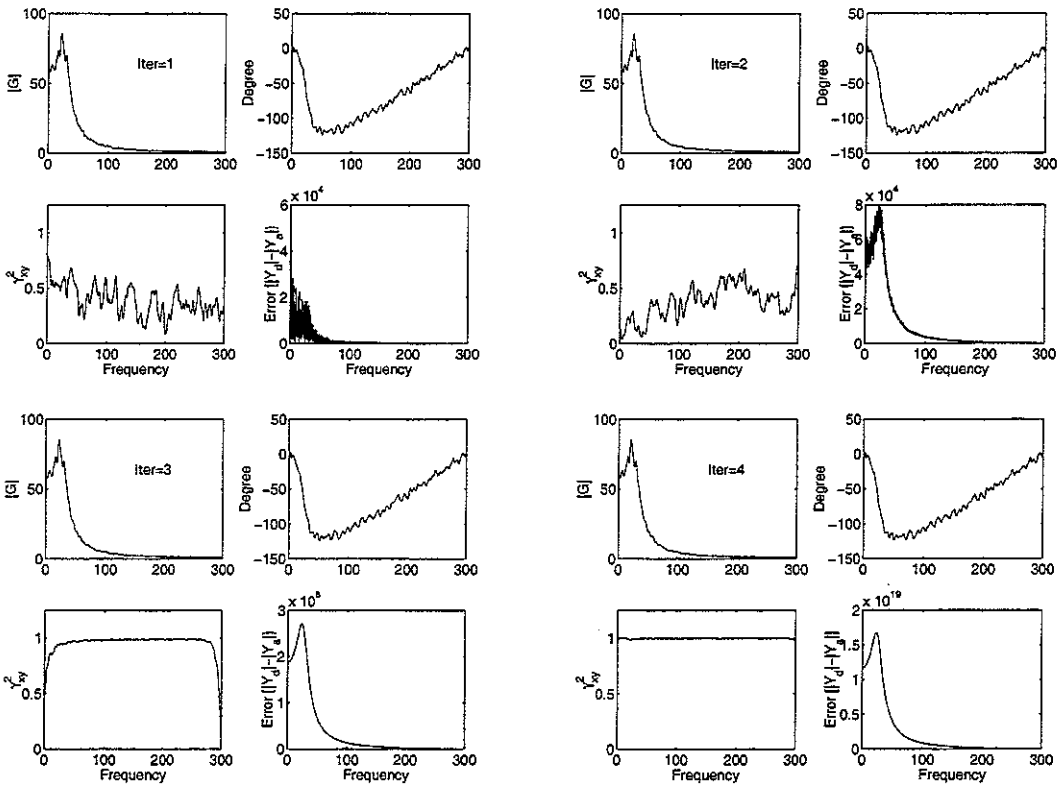

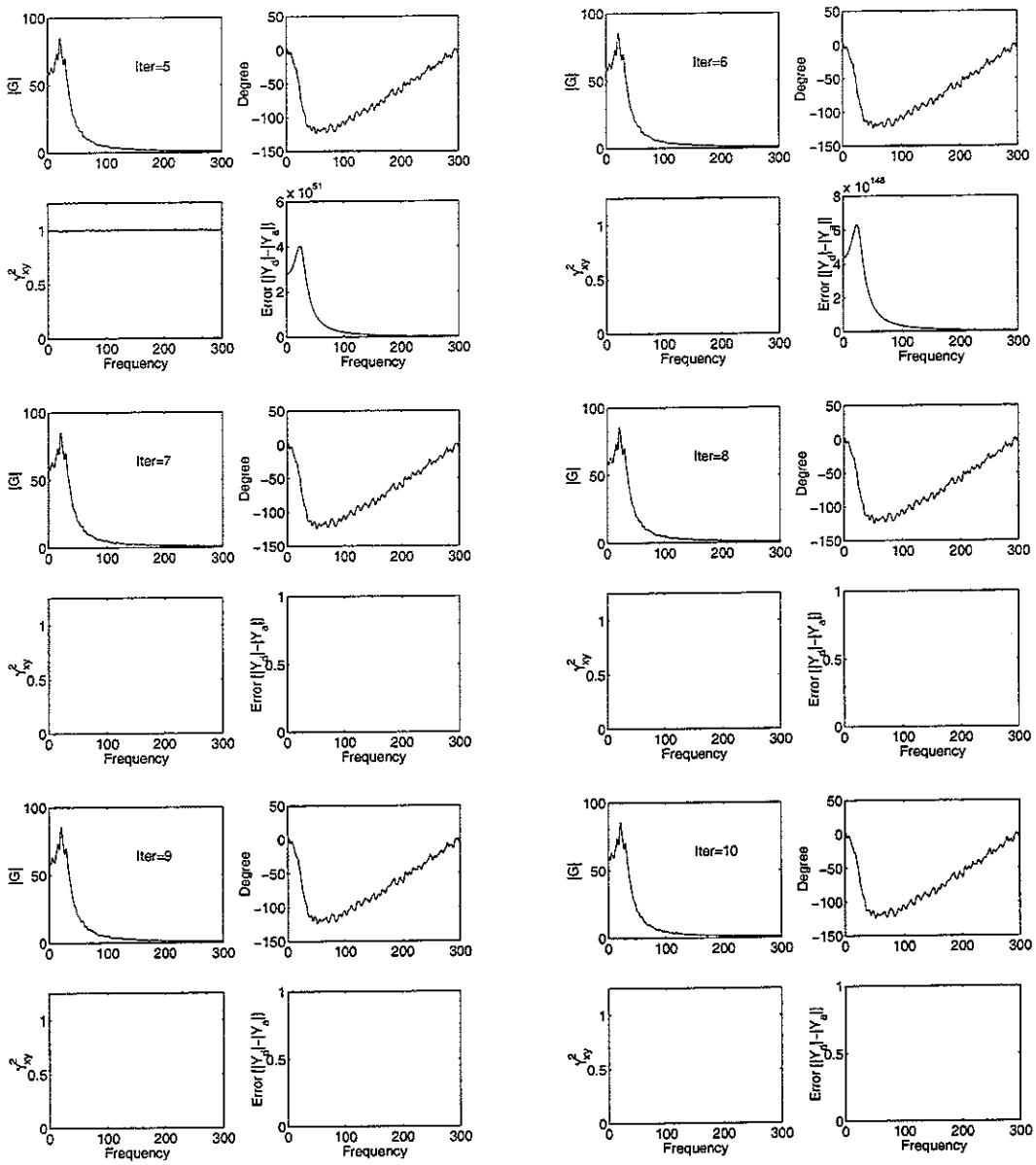

Result of the input signal reconstruction and change of error

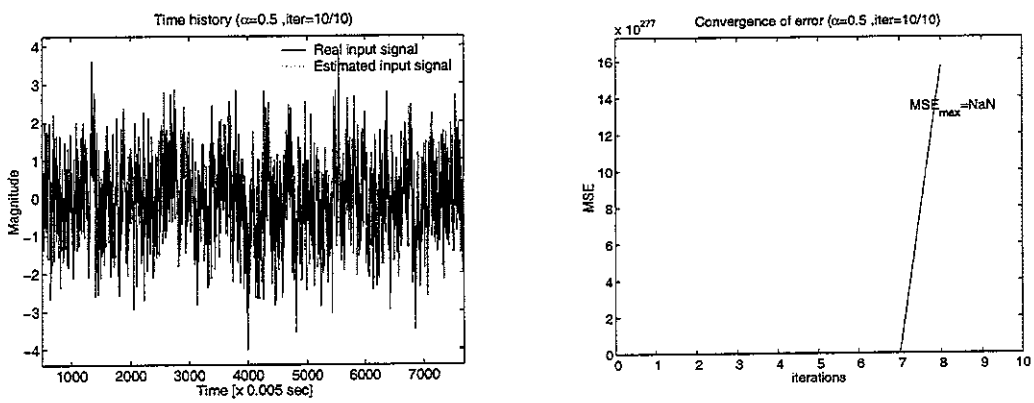

Changes of frequency response and coherence function for cubic non-linear system ($y = x + \delta x^3$ with $\delta = 1.0$) with dynamics (new method)

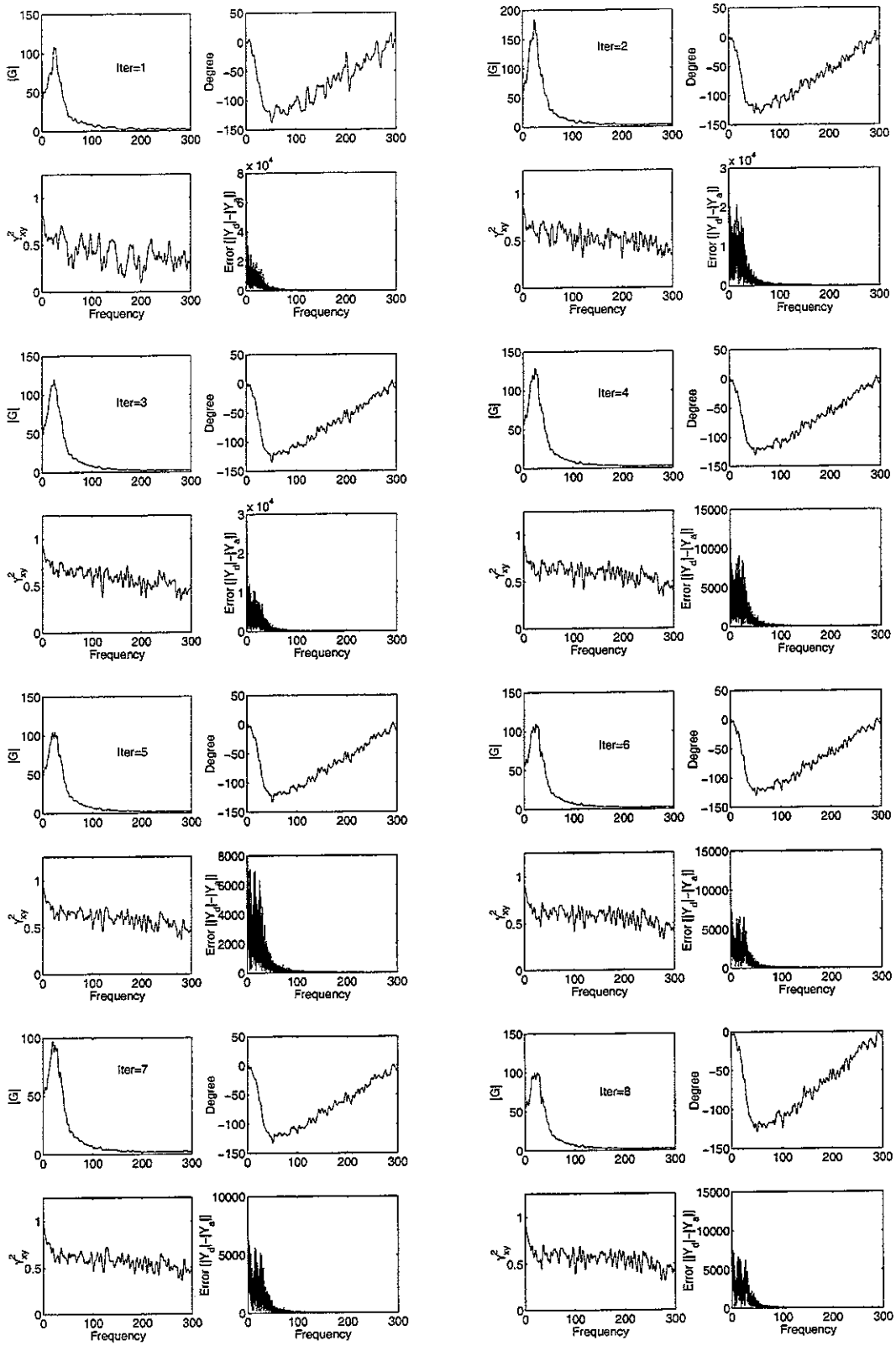

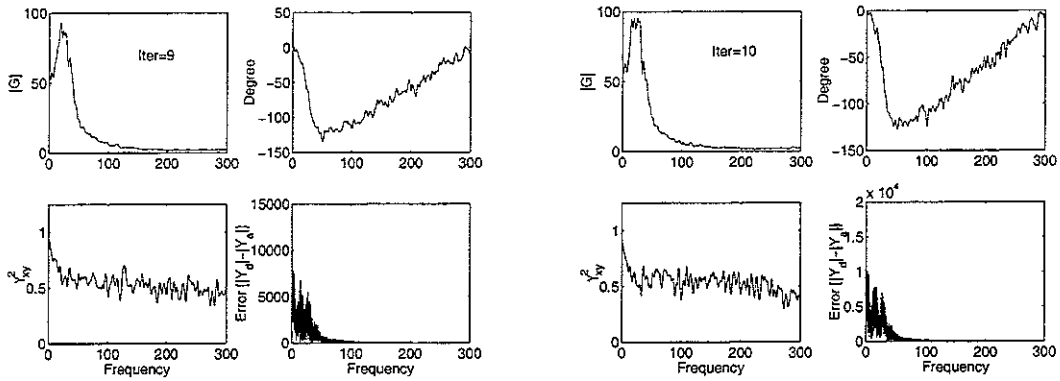

Result of the input signal reconstruction and change of error

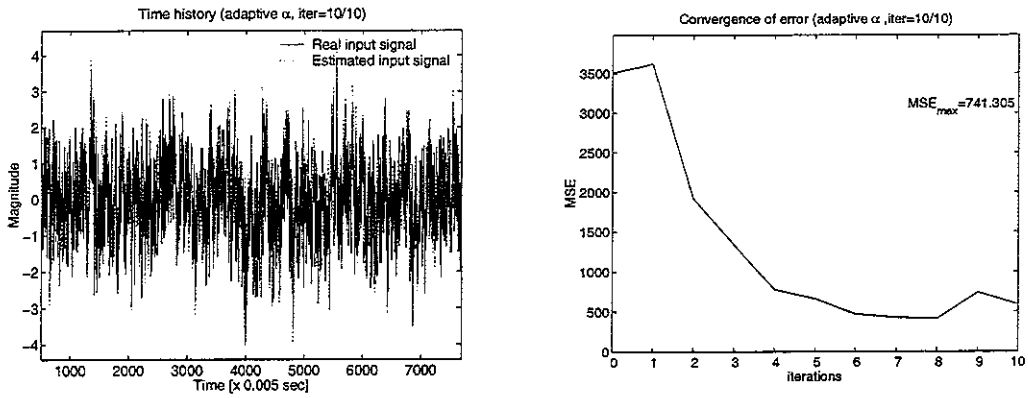

Simulation 2: Changes of frequency response and coherence function for hyperbolic non-linear system $(y = -\tanh(-x \cdot (0.09 - x^2))^2)$ with dynamics (conventional method)

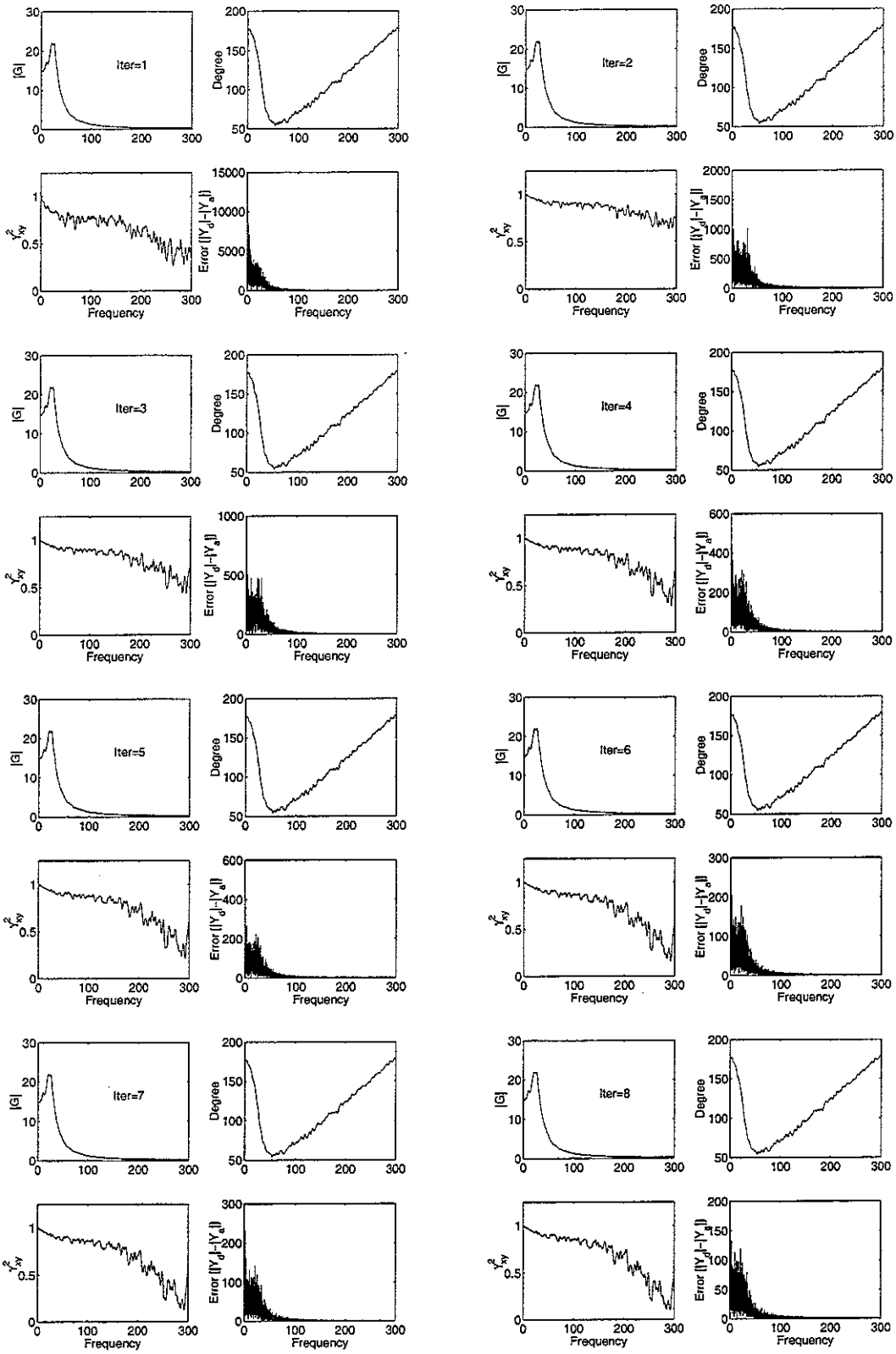

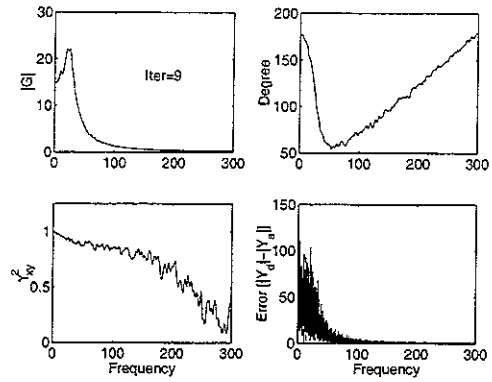

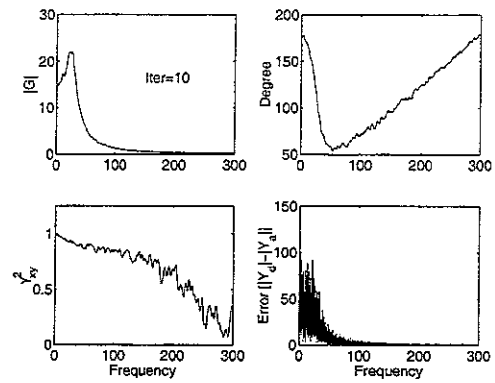

Result of the input signal reconstruction and change of error

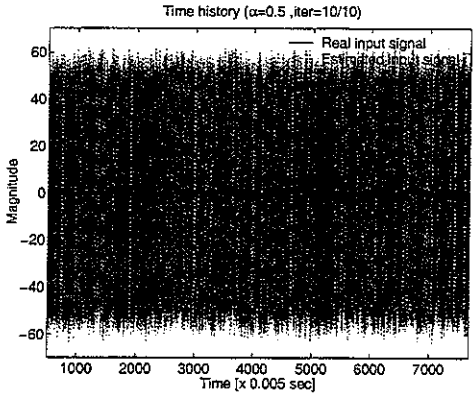

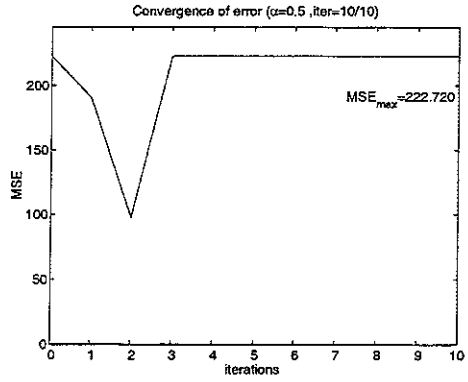

Changes of frequency response and coherence function for hyperbolic non-linear system ($y = -\tanh(-x \cdot (0.09 - x^2))^2$) with dynamics (new method)

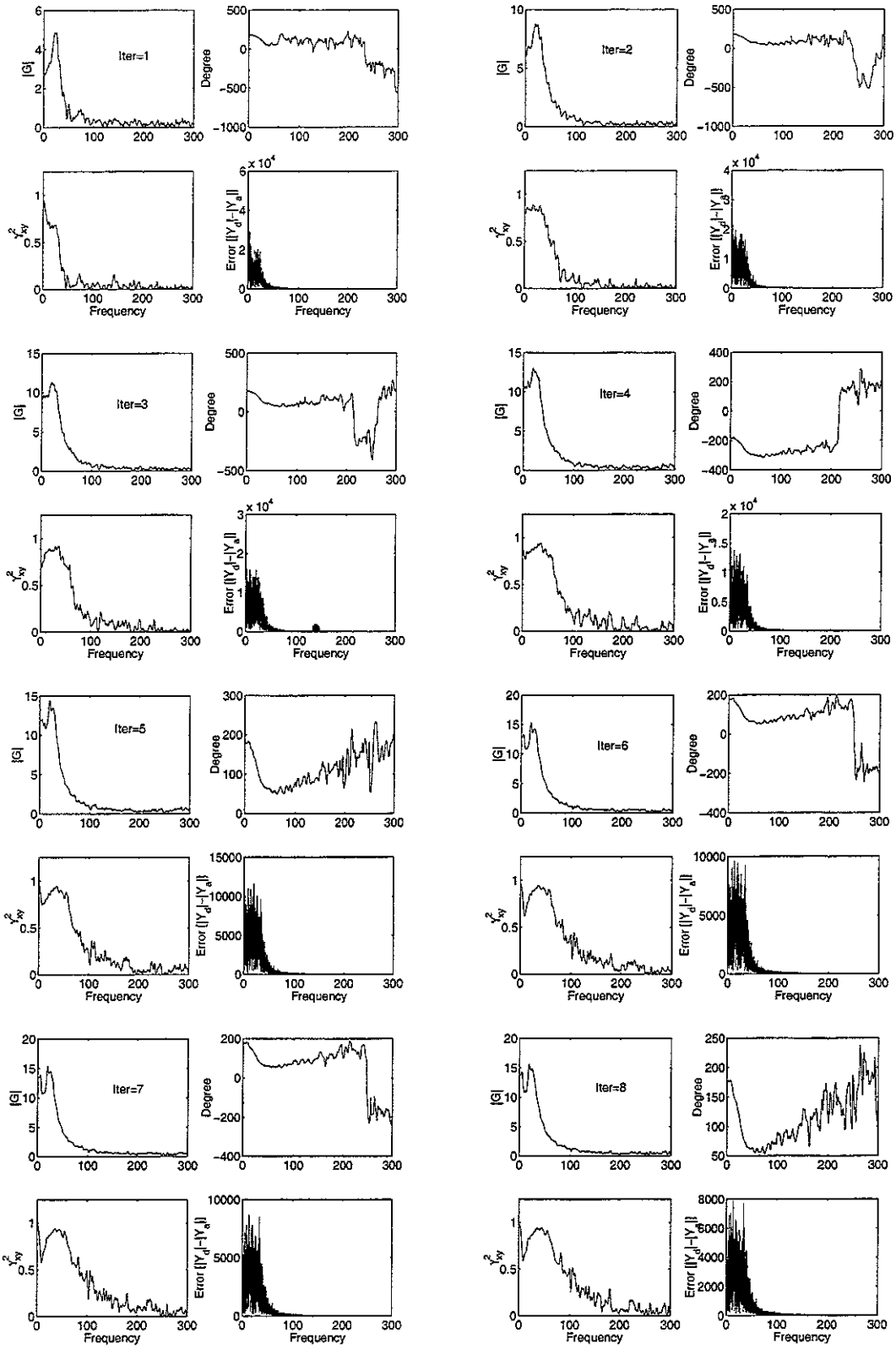

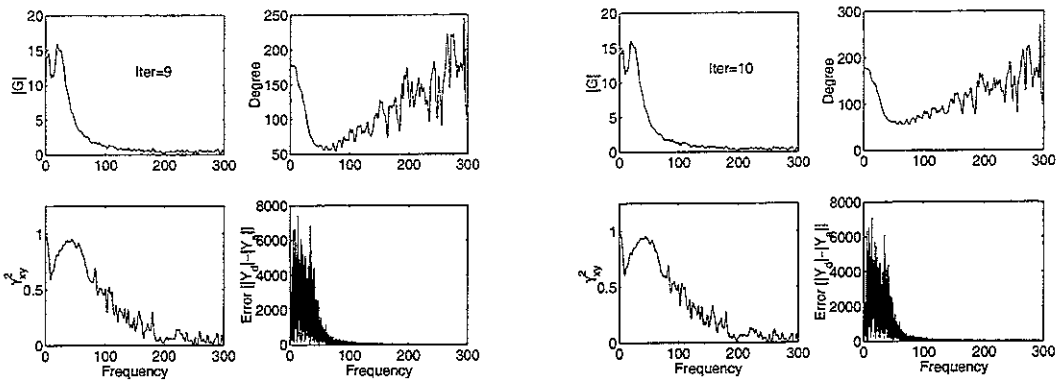

Result of the input signal reconstruction and change of error

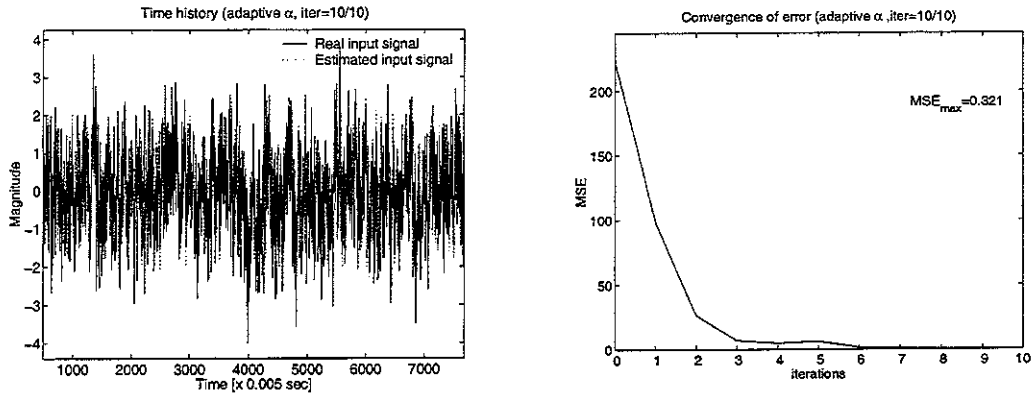

Table C.1 Summary of simulation results

Model	Methods for IL process	Stability	MSE(between input signal and restored signal)	Remarks on the input signal reconstruction
Cubic **Nonlinear system**	Conventional method	×	-	Unsuccessful
	Modified (new) method	o	0.32	Successful
Hyperbolic **Nonlinear system**	Conventional method	-	2936.39	Unsuccessful
	Modified (new) method	o	0.09	Successful (amplitude of the restored signal is slightly limited)

C.2 Nonlinear car model

Key parameters;

Sample length (N) : 8192 samples with input signal pink noise ($\sigma_x^2 = 1$)

Sampling frequency (f_s) : 200 Hz

Fixed gain factor (α) : 0.5

Window : Hanning 256 segments

Averaging : 50 % overlapping

Number of iterations : 10

Changes of frequency response and coherence function for 1/4 car model with non-linear damper (conventional method)

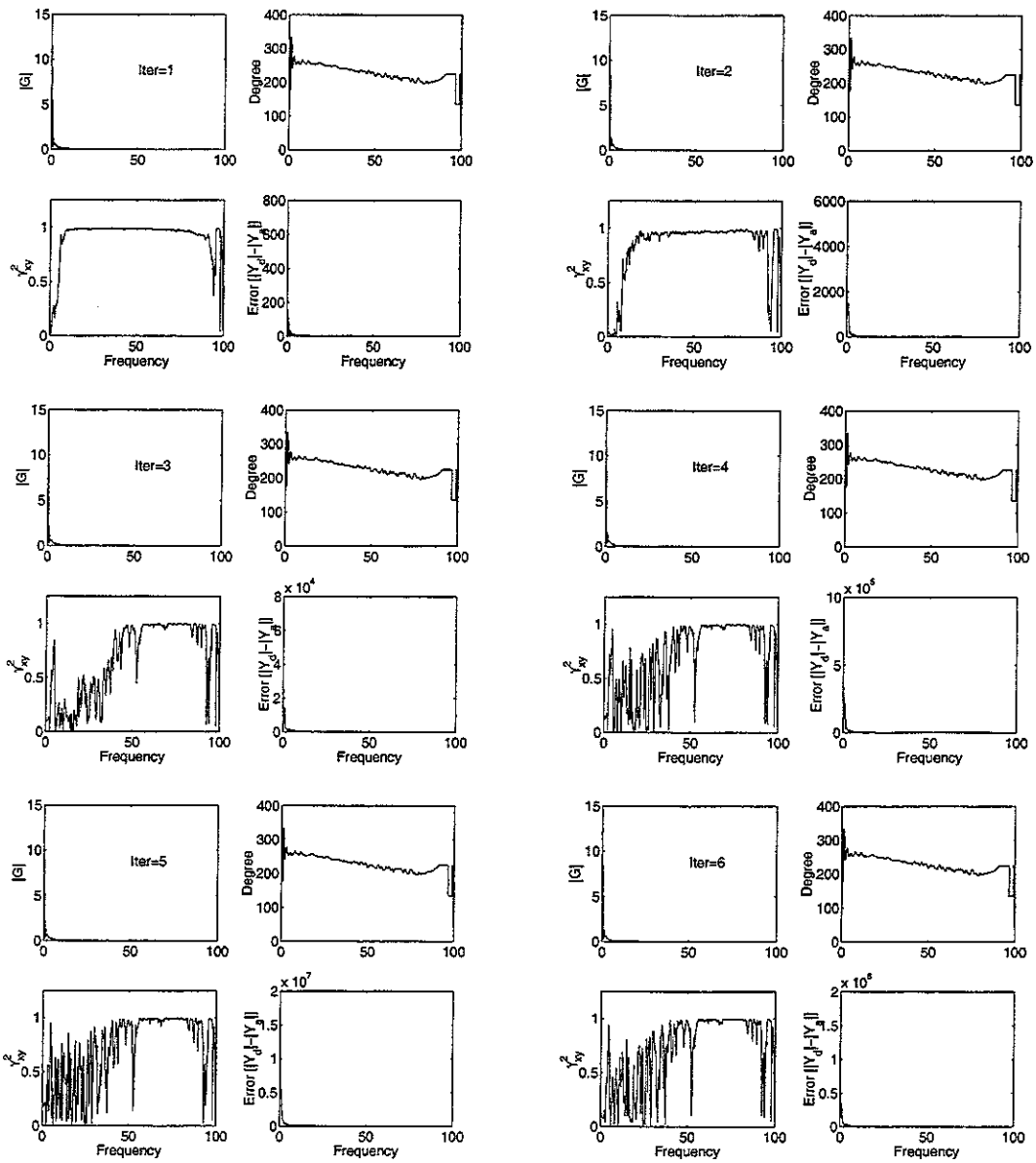

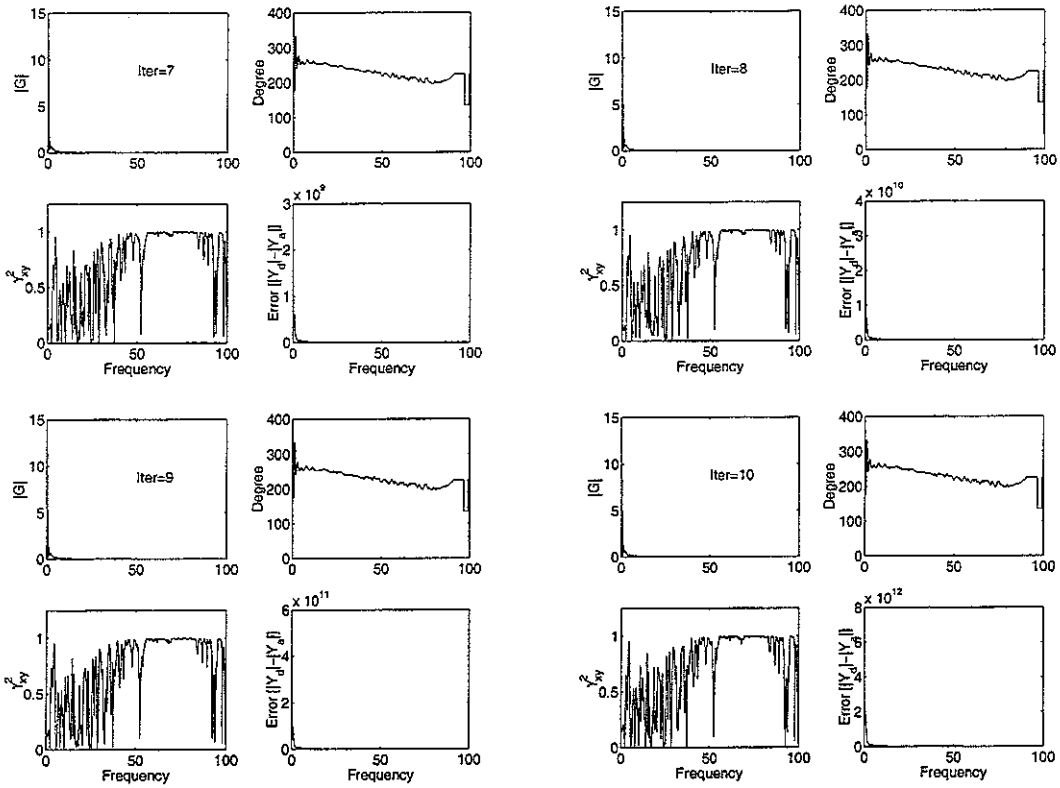

Change of error and result of the input signal reconstruction

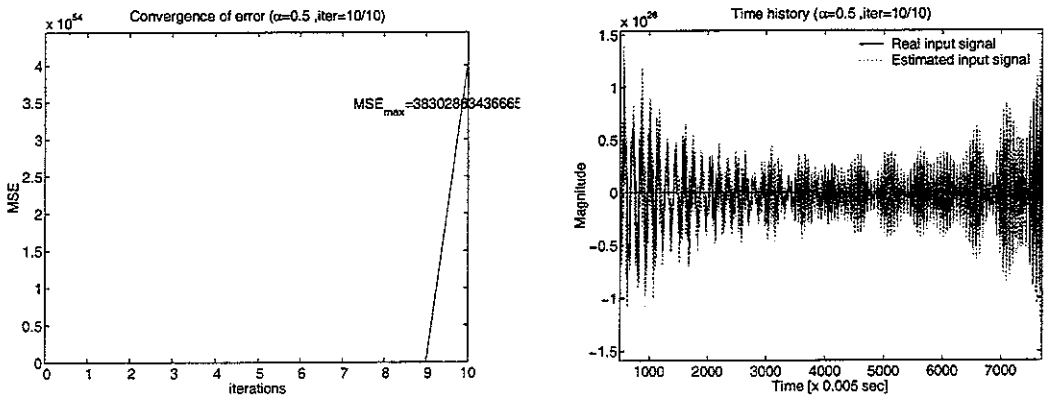

Changes of frequency response and coherence function for 1/4 car model with non-linear damper (new method)

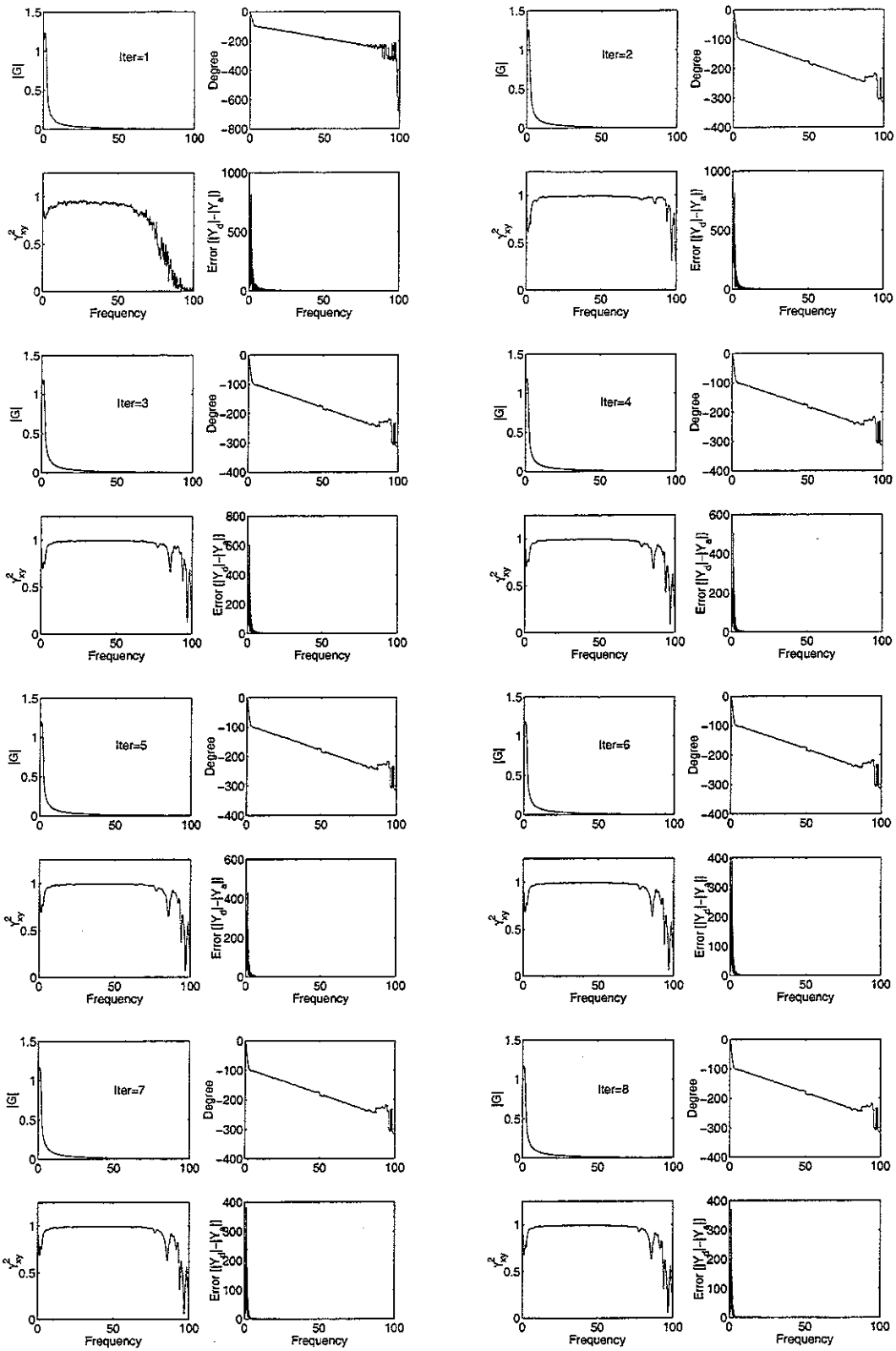

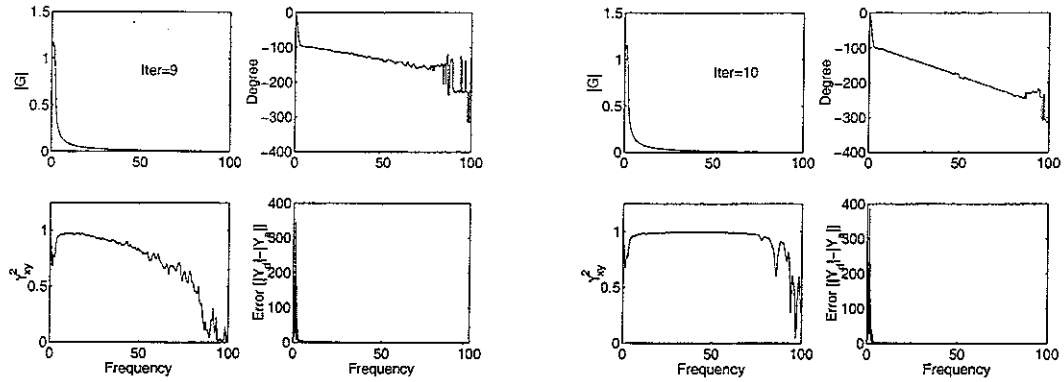

Change of error and result of the input signal reconstruction